5 Application of Composite Filter for PQ issues in Distribution Network

5.1 Introduction

This chapter deals with an application of composite filter to EAF distribution network for PQ issues using Matlab-Simulink platform to verify the proposed control. Each power device has been modeled using the SimPowerSystem toolbox library.

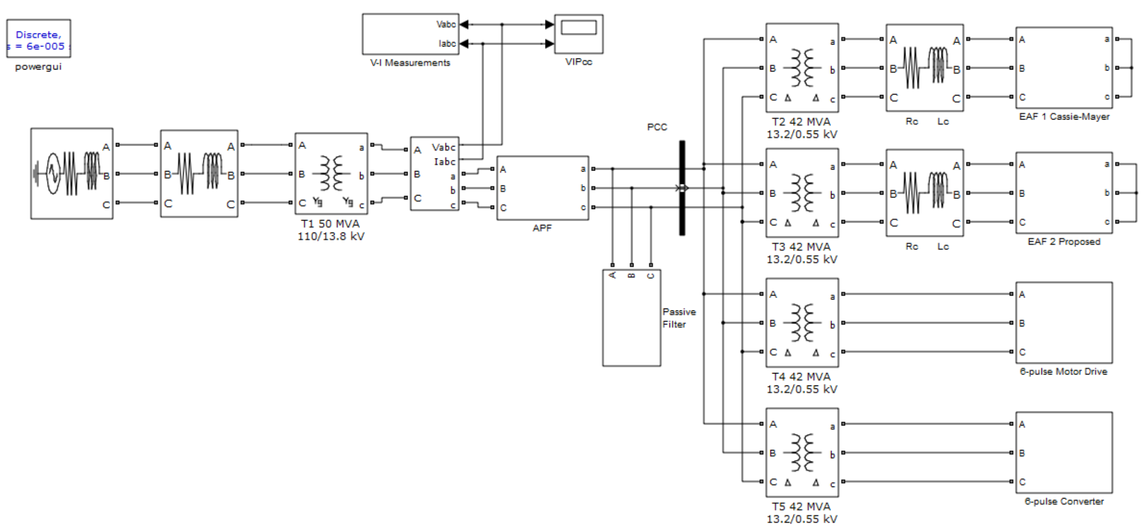

Figure 5.1 Complete MATLAB simulation file of composite filter connected to EAF network

Figure 5.1 shows complete Simulink/MATLAB file of test system shown in Figure 2.46. The distribution network consists of EAF-1-Cassie-Mayer model and EAF-2-Proposed model along with the auxiliaries. EAF is modeled as a non-linear time varying voltage controlled source using subsystem/MATLAB. The arc current is taken as the input parameter to this function and the output is non-linear time varying voltage.

5.2 Performance analysis of CF

Performance evaluation of CF for PQ issues in an EAF connected distribution network is carried out for various operational cycles of the EAF, which includes-analysis in refining cycle, analysis in melting cycle (sinusoidal flicker), analysis in melting cycle (random cycle) and unbalanced voltage analysis. The performance of EAF in various cycles is discussed in the following sub-sections:

5.2.1 Performance analysis of CF in refining cycle

Figure 5.2 shows filter performance in refining cycle of the EAF connected distribution network. Figure 5.2 (a)-(c)-(e) shows V_{PCC} waveforms without filter, with PF and with CF respectively. Figure 5.2 (b)-(d)-(f) shows harmonic spectrum of V_{PCC} without filter, with PF and with CF respectively.

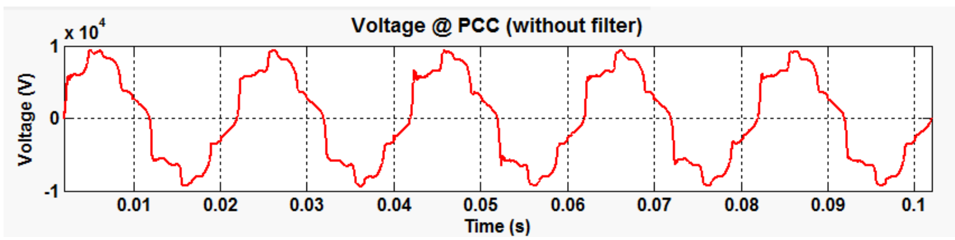

(a)

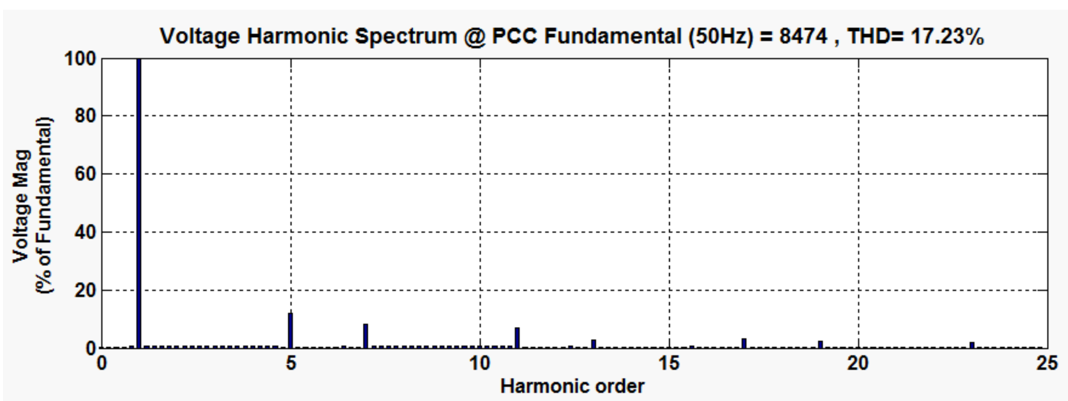

(b)

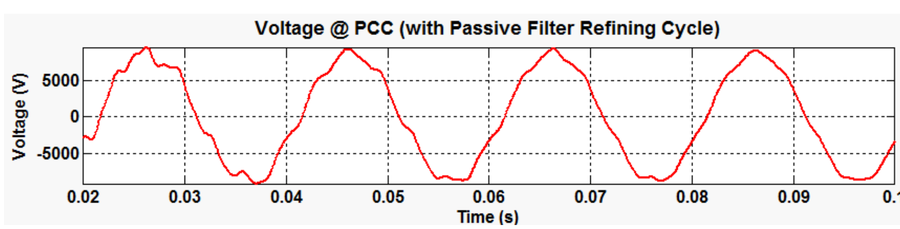

(c)

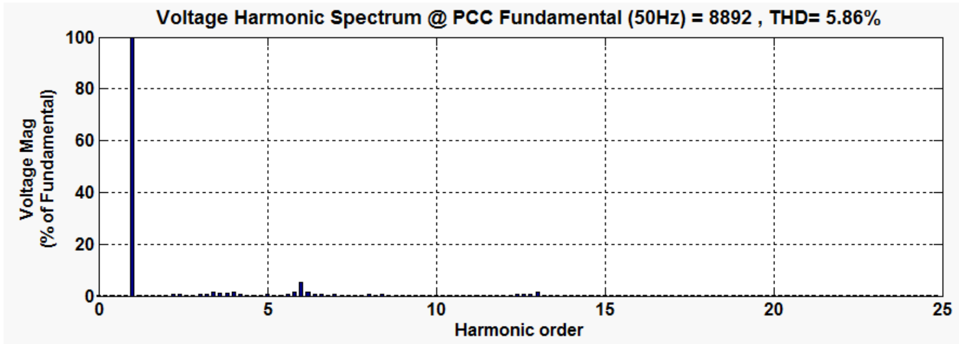

(d)

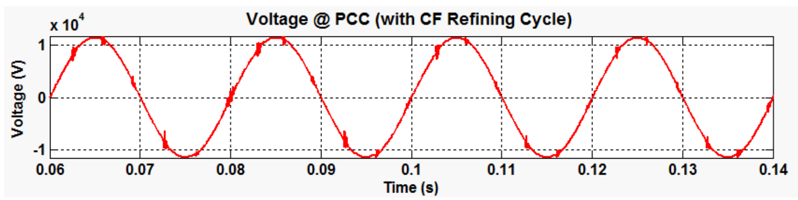

(e)

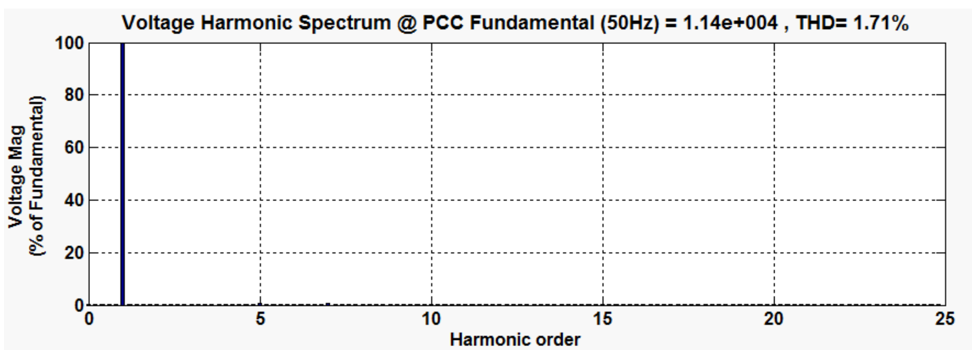

(f)

Figure 5.2 Filter performance in EAF refining cycle (a) V_{PCC} without filter (b) harmonic spectrum without filter (c) V_{PCC} with PF (d) harmonic spectrum with PF (e) V_{PCC} with CF (f) harmonic spectrum with CF

The total harmonic distortion of voltage (THD_V) observed at PCC is 17.23 % without filter in refining cycle of EAF connected distribution network as shown in Figure 5.2 (b). This value is violating IEEE 519-1992 limits. It should be below 5%. That is improved to 5.86 % after passive filter application as shown in Figure 5.2(d), which is still violating IEEE 519-1992.Application of CF changes THD_V to 1.71 % as shown in Figure 5.2 (f).

Table 5.1 shows three phase harmonic spectrum details of voltage and current at PCC for refining cycle of the EAF connected distribution network.

Table 5.1 Harmonic analysis of EAF connected distribution network in refining cycle

Parameters/condition	Phase	V/I	THD (%)	RMS	Fund.	H_5 (%)	H_7 (%)	H_{11} (%)	H_{13} (%)
Without filter	Phase-a	V	17.23	5992	8474	11.99	8.27	6.98	2.59
		I	4.74	1374	1943	4.06	2	0	0
	Phase-b	V	17.49	5976	8451	12.29	8.36	7.24	2.73
		I	4.73	1387	1962	4.11	2	1.1	0
	Phase-c	V	17.47	5979	8456	12.26	8.31	7.28	2.73
		I	4.72	1388	1963	4.09	1.99	1.1	0
With PF	Phase-a	V	5.86	6288	8892	0.58	0.47	0.09	1.26
		I	1.72	1413	1999	0.18	0.11	0	0
	Phase-b	V	2.73	6271	8869	0.65	0.33	0.11	0.94
		I	0.82	1413	1997	0.22	0.05	0	0
	Phase-c	V	4.96	6292	8898	0.68	0.23	0.07	0.54
		I	1.54	1405	1987	0.25	0.06	0	0
With CF	Phase-a	V	1.71	8064	1140	0.64	0.44	0.21	0.18
		I	3.88	106.3	150.3	3.33	1.68	0.52	0.31
	Phase-b	V	1.92	8067	11410	0.67	0.44	0.24	0.16
		I	4.33	105.1	148.6	3.74	1.76	0.61	0.35
	Phase-c	V	1.92	8067	11410	0.65	0.43	0.24	0.13
		I	4.29	105.1	148.7	3.6	1.77	0.69	0.3

It can be seen that 5th, 7th, 11th and 13th are the major harmonic components present in voltage at PCC. H_5, H_7 and H_{11} are more than IEEE 519-1992 limit of 5 % of harmonic distortion. It can be seen from Table 5.2 that both PF and CF can suppress individual harmonic components within the limit in refining cycle of EAF distribution network at PCC.

Figure 5.3 shows filter performance in refining cycle of the EAF connected network. Figure 5.3 (a)-(c)-(e) shows I_{PCC} waveforms without filter, with PF and with CF respectively. Figure 5.3 (b)-(d)-(f) shows harmonic spectrum of I_{PCC} without filter, with PF and with CF respectively.

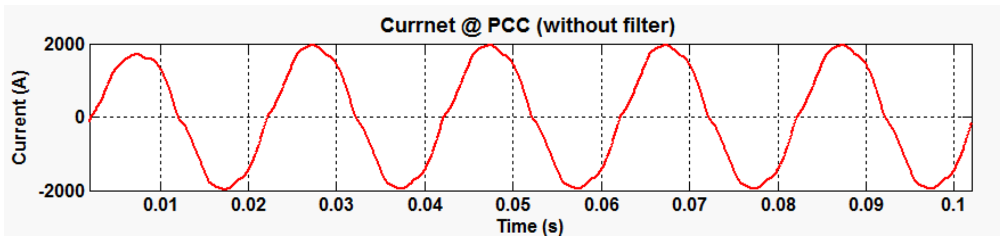

(a)

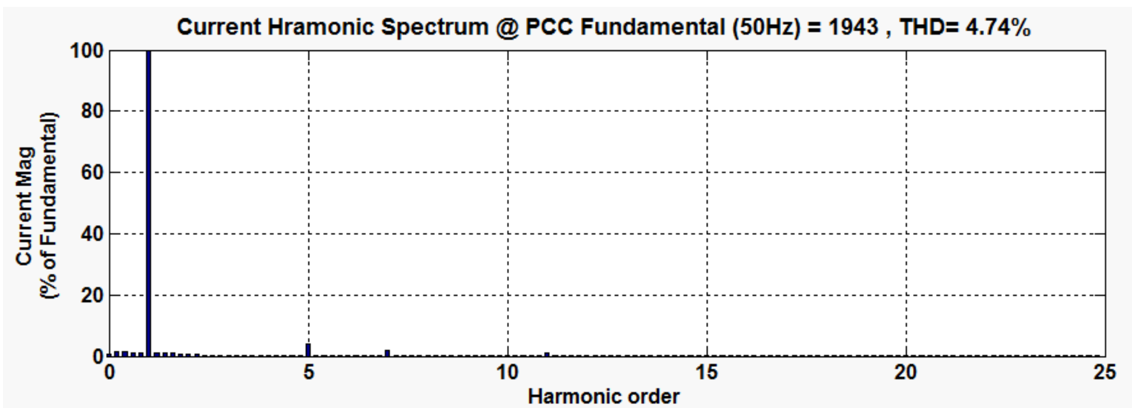

(b)

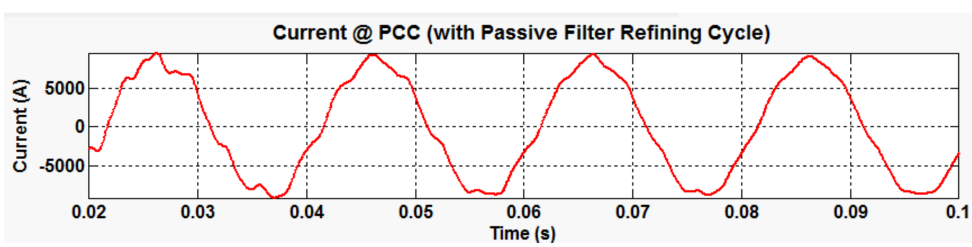

(c)

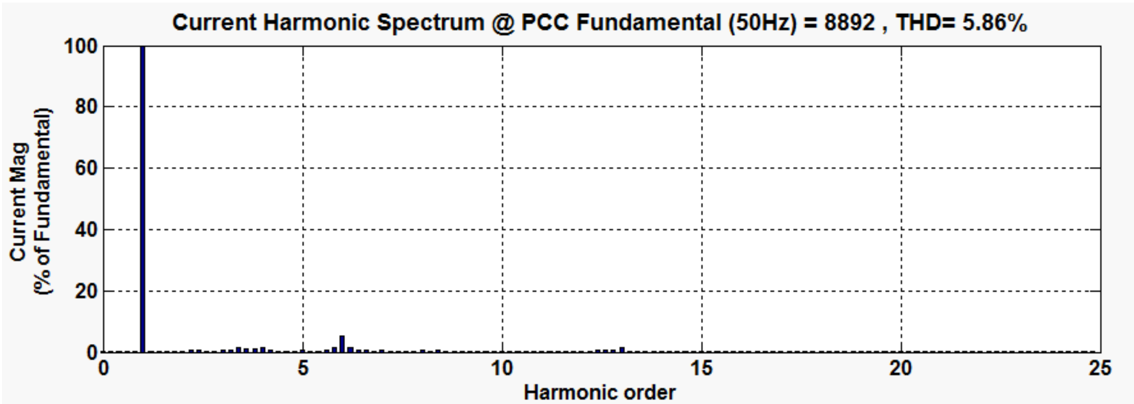

(d)

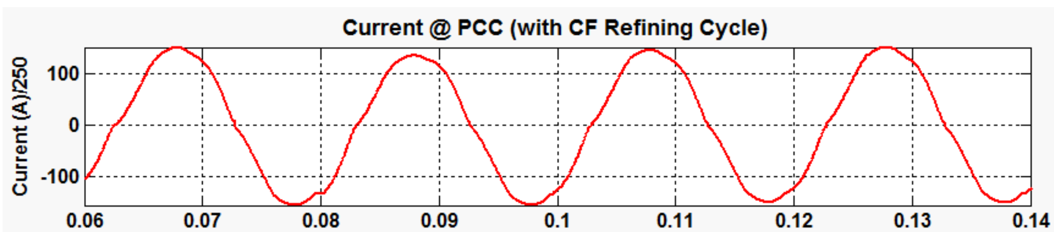

(e)

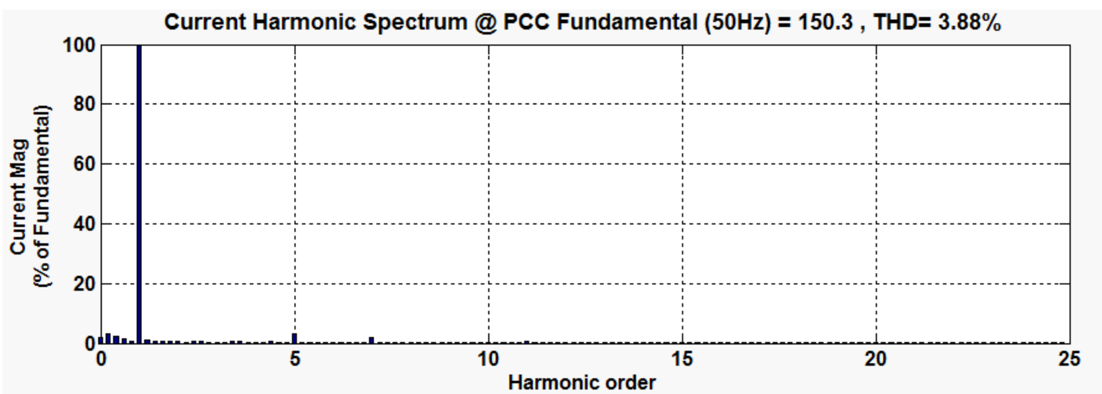

(f)

Figure 5.3 Filter performance in EAF refining cycle (a) I_{PCC} without filter (b) harmonic spectrum without filter (c) I_{PCC} with PF (d) harmonic spectrum with PF (e) I_{PCC} with CF (f) harmonic spectrum with CF

The total harmonic distortion of current (THD_I) observed at PCC is 4.74 % without filter in refining cycle of EAF connected distribution network as shown in Figure 5.3 (b). It has improved to 1.72 % and then changes to 3.82 % after PF and CF application as shown in Figure 5.3 (d) and (f) respectively, which are within the permissible limits. Harmonics spectrum quantified detail is tabulated in Table 5.1.It shows that PF performs better than CF in reducing THD_I in refining cycle.

It can be noted that 5^{th}, 7^{th}, $11^{th}$and 13^{th} are the major harmonic components present in current at PCC. H_5, H_7 and H_{11} are more than IEEE 519-1992 limit of 5 % of harmonic distortion. It can be seen that 5^{th}, 7^{th}, 11^{th} and 13^{th} are the major harmonic components present in voltage at PCC. $H_5$is more than IEEE 519-1992 limit of 5 % of harmonic distortion.

It can be seen from Table 5.1 that both PF and CF can suppress individual harmonic component within the limit in refining cycle of EAF distribution network at PCC

Figure 5.4 (a)-(d)-(g) depicts typical VICs without filter, with PF and with CF application respectively. Figure 5.4 (b)-(e)-(h) shows active-reactive-apparent power consumption at PCC by the EAF distribution network without filter, with PF and with CF application respectively.

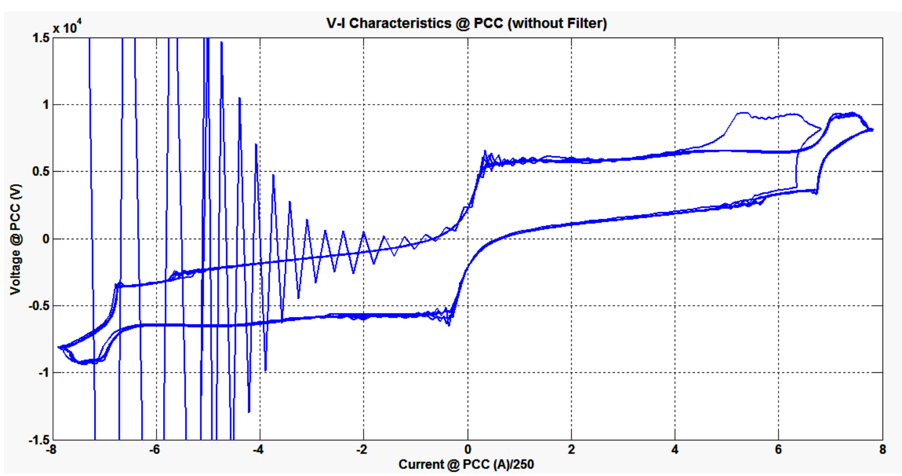

(a)

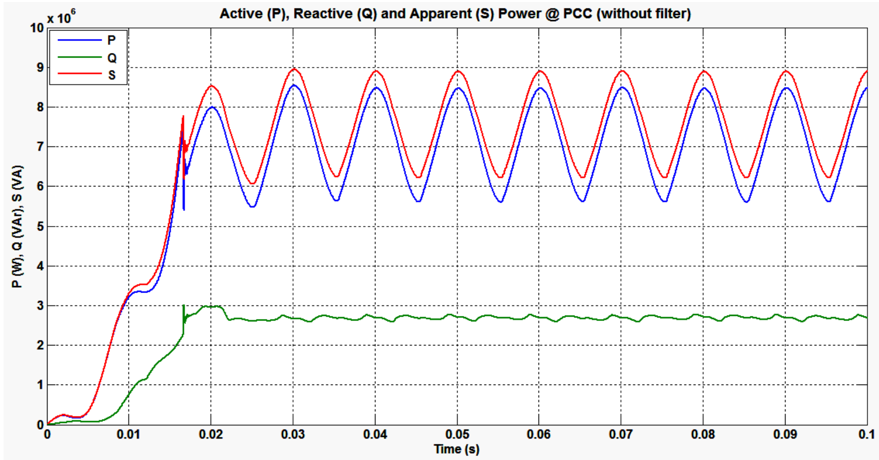
Active (P), Reactive (Q) and Apparent (S) Power @ PCC (without filter)
x 10^6
P
Q
S
P (W), Q (VAr), S (VA)
Time (s)

(b)

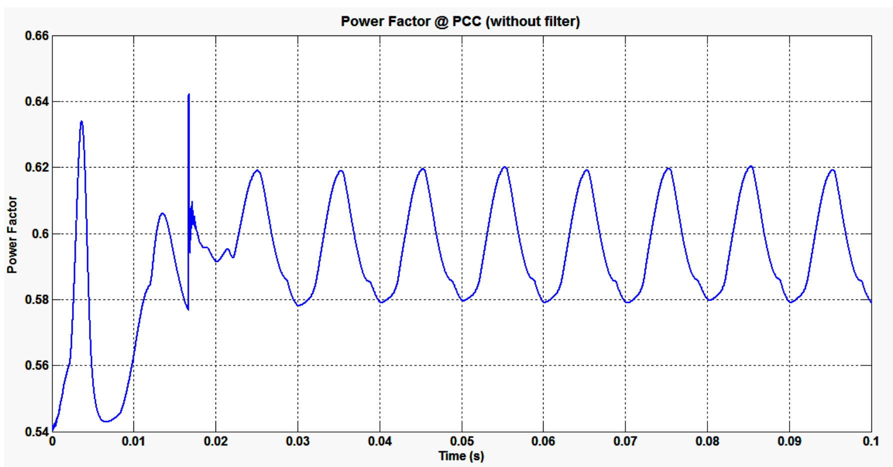
Power Factor @ PCC (without filter)
Power Factor
Time (s)

(c)

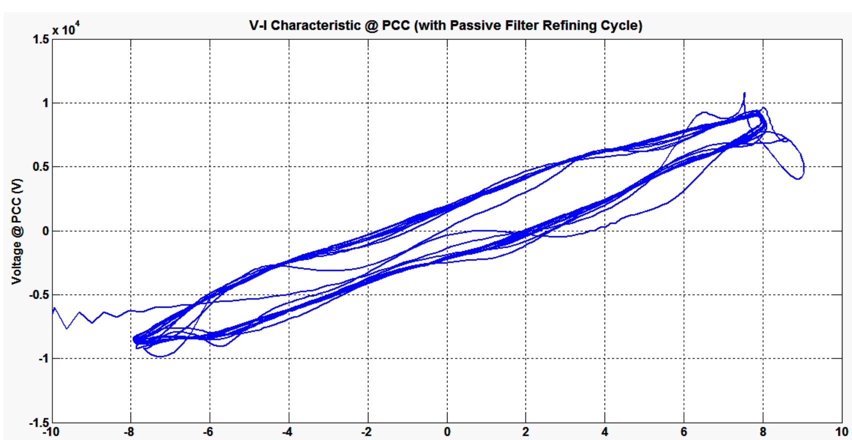
V-I Characteristic @ PCC (with Passive Filter Refining Cycle)
x 10^4
Voltage @ PCC (V)
Current @ PCC (A)/250

(d)

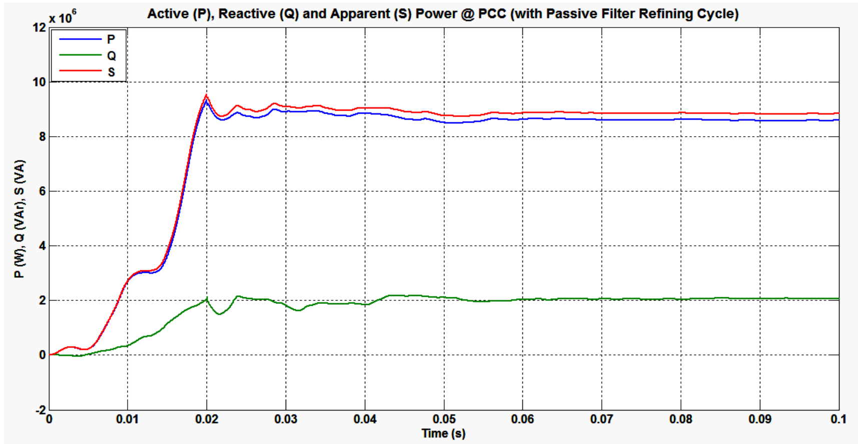
Active (P), Reactive (Q) and Apparent (S) Power @ PCC (with Passive Filter Refining Cycle)
x 10^6
P
Q
S
P (W), Q (VAr), S (VA)
Time (s)

(e)

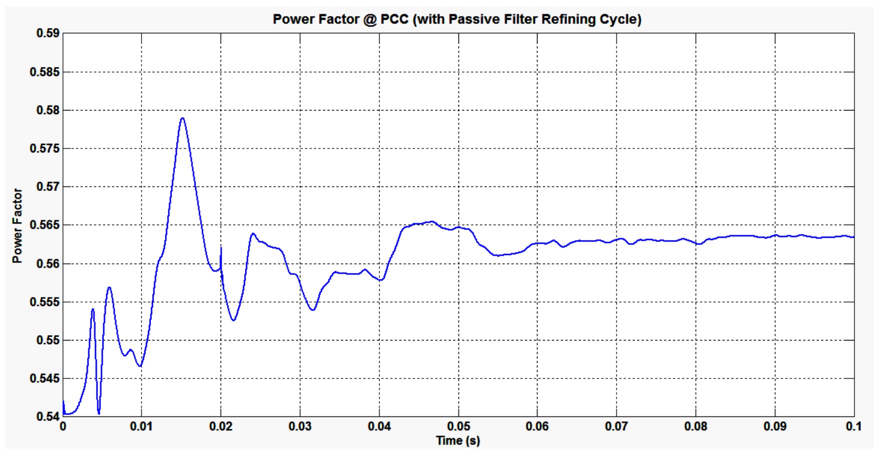
Power Factor @ PCC (with Passive Filter Refining Cycle)
Power Factor
Time (s)

(f)

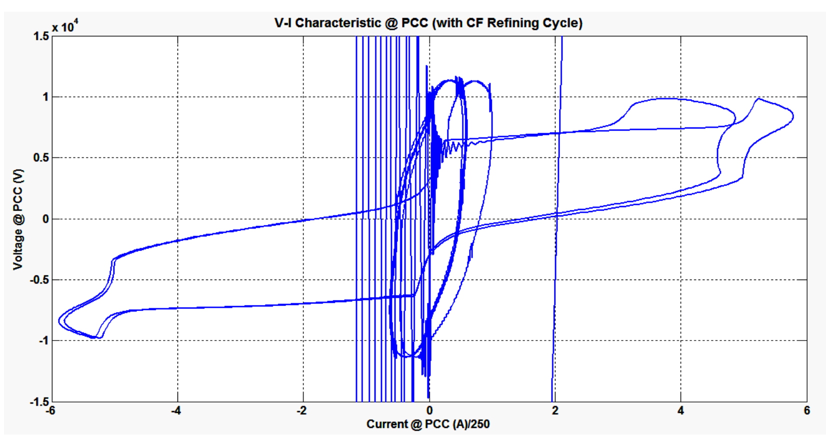
V-I Characteristic @ PCC (with CF Refining Cycle)
x 10^4
Voltage @ PCC (V)
Current @ PCC (A)/250

(g)

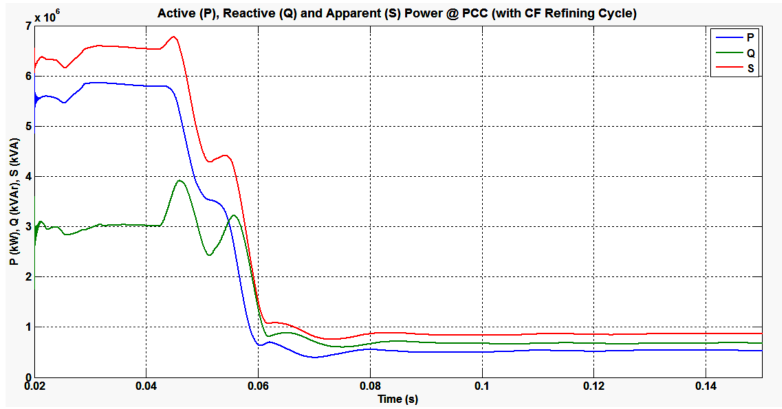

(h)

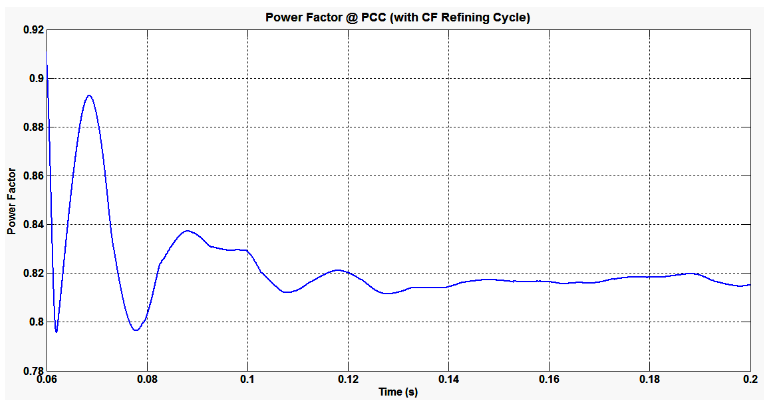

(i)

Figure 5.4 Filter performance in EAF refining cycle (a) VIC without filter (b) PQS powers without filter (c) power factor without filter (d) VIC with PF (e) PQS powers with PF (f) power factor with PF (g) VIC with CF (h) PQS powers with CF (i) power factor with CF

Figure 5.4 (c)-(f)-(i) shows power factor variation without filter, with PF and with CF application respectively at PCC. Table 5.2 shows tabulated values of active-reactive-apparent power and power factor after PF and CF application.

It can be seen from Table 5.2 that the power factor without filter is 0.59 which is improved to 0.56 and then to 0.82 after PF and CF application respectively in refining cycle of the EAF distribution network at PCC. It means CF performs better than PF alone in power factor improvement.

Table 5.2 Power analysis in refining cycle

Parameters/condition	Phase	P (kW)	Q (kVAr)	S (kVA)	pf
Without filter	Phase-a	7131	2682	7627	0.59
	Phase-b	7054	2642	7541	0.59
	Phase-c	7106	2693	7607	0.59
With PF	Phase-a	8602	2056	8844	0.56
	Phase-b	8595	2060	8839	0.56
	Phase-c	8588	2063	8833	0.56
With CF	Phase-a	5227	6945	8701	0.82
	Phase-b	5718	7195	9238	0.81
	Phase-c	5263	7416	9183	0.82

5.2.2 Performance analysis of CF in melting cycle (sinusoidal flicker)

Figure 5.5 shows filter performance in melting cycle considering sinusoidal flicker of the EAF connected distribution network. Figure 5.5 (a)-(c)-(e) shows V_{PCC} waveforms without filter, with PF and with CF respectively. Figure 5.2 (b)-(d)-(f) shows harmonic spectrum of V_{PCC} without filter, with PF and with CF respectively.

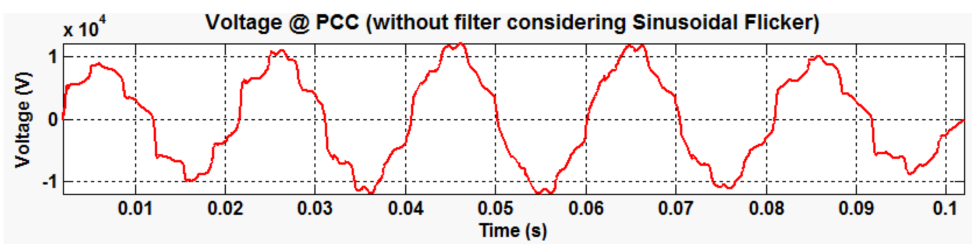

(a)

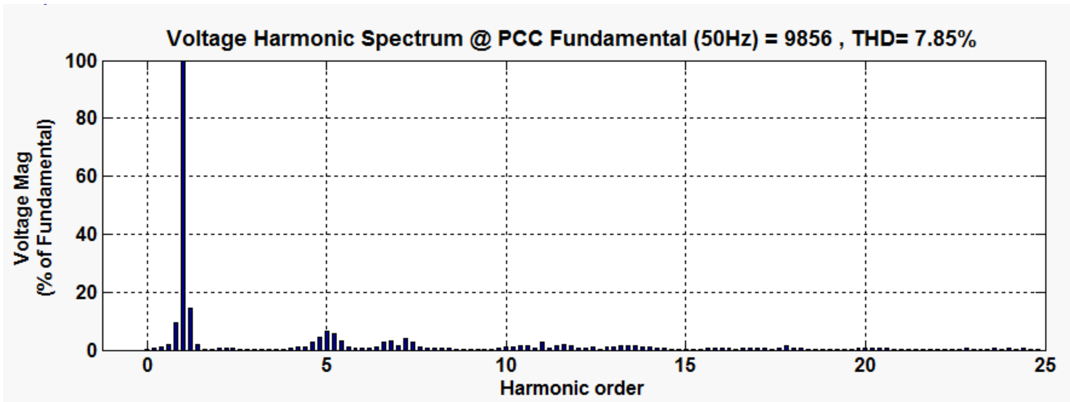
Voltage Harmonic Spectrum @ PCC Fundamental (50Hz) = 9856 , THD= 7.85%
Voltage Mag
(% of Fundamental)
Harmonic order
100
80
60
40
20
0
0
5
10
15
20
25

(b)

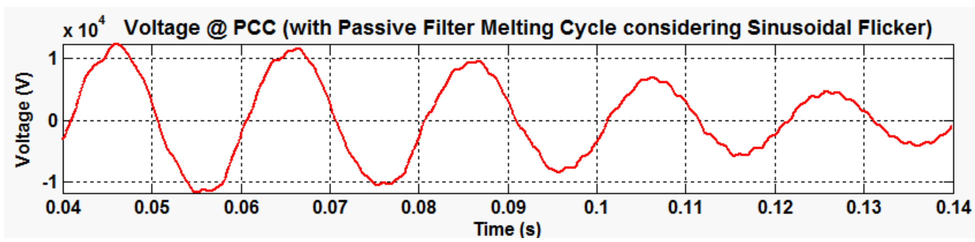
x 10^4
Voltage @ PCC (with Passive Filter Melting Cycle considering Sinusoidal Flicker)
Voltage (V)
Time (s)
1
0
-1
0.04
0.05
0.06
0.07
0.08
0.09
0.1
0.11
0.12
0.13
0.14

(c)

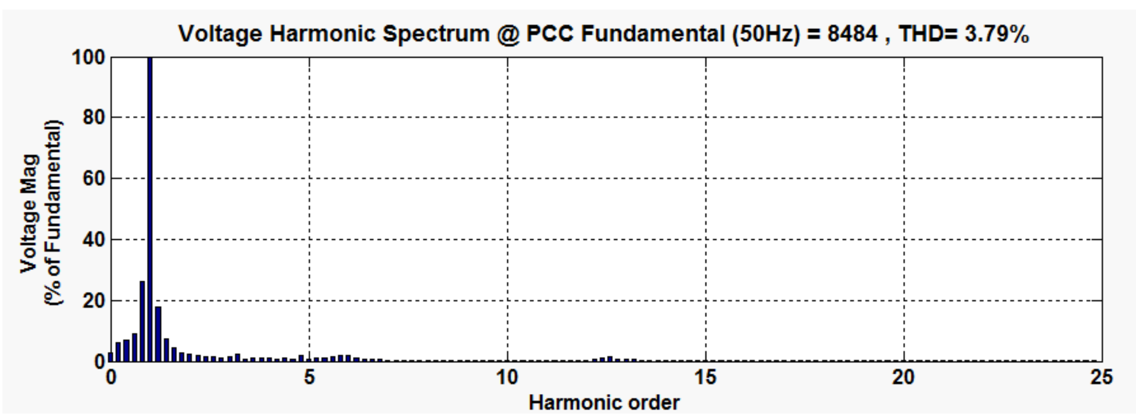
Voltage Harmonic Spectrum @ PCC Fundamental (50Hz) = 8484 , THD= 3.79%
Voltage Mag
(% of Fundamental)
Harmonic order
100
80
60
40
20
0
0
5
10
15
20
25

(d)

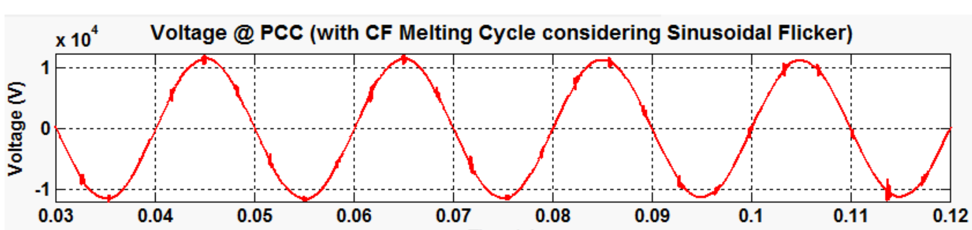
x 10^4
Voltage @ PCC (with CF Melting Cycle considering Sinusoidal Flicker)
Voltage (V)
Time (s)
1
0
-1
0.03
0.04
0.05
0.06
0.07
0.08
0.09
0.1
0.11
0.12

(e)

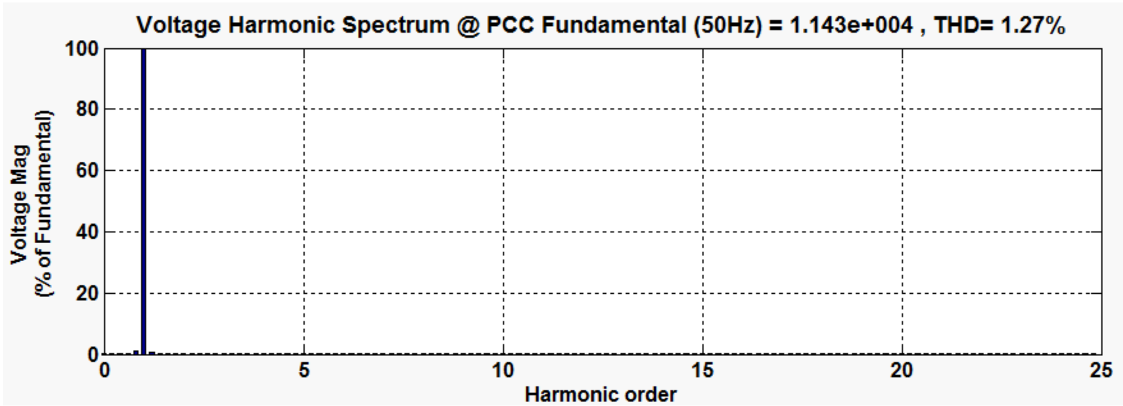

(f)

Figure 5.5 Filter performance in EAF melting cycle (sinusoidal flicker) (a) V_{PCC} without filter (b) harmonic spectrum without filter (c) V_{PCC} with PF (d) harmonic spectrum with PF (e) V_{PCC} with CF (f) harmonic spectrum with CF

The total harmonic distortion of voltage (THD_V) observed at PCC is 7.85 % without filter in melting cycle considering sinusoidal flicker of EAF connected distribution network as shown in Figure 5.2 (b). This value is violating IEEE 519-1992 limits. It should be below 5%. That is improved to 3.79 % after passive filter application as shown in Figure 5.2 (d), which is within the IEEE 519-1992. An application of series APF along with passive filter changes THD_v to 1.27 % as shown in Figure 5.2 (f). That means CF performs better than the PF in improving THD_V in melting cycle considering sinusoidal flicker of EAF connected distribution network.

Table 5.3 show three phase harmonic spectrum details of voltage and current at PCC respectively for melting cycle considering sinusoidal flicker of the EAF connected distribution network. It can be seen that 5^{th}, 7^{th}, 11^{th} and 13^{th} are the major harmonic components present in voltage at PCC. $H_5$is more than IEEE 519-1992 limit of 5 % of harmonic distortion. It can be seen from Table 5.2 that both PF and CF can suppress individual harmonic components within the limit in melting cycle (sinusoidal flicker) of EAF distribution network at PCC but CF performs better than the PF.

Figure 5.6 shows filter performance in melting cycle considering sinusoidal flicker of the EAF connected network. Figure 5.3 (a)-(c)-(e) shows I_{PCC} waveforms without filter, with

PF and with CF respectively. Figure 5.3 (b)-(d)-(f) shows harmonic spectrum of I_{PCC} without filter, with PF and with CF respectively.

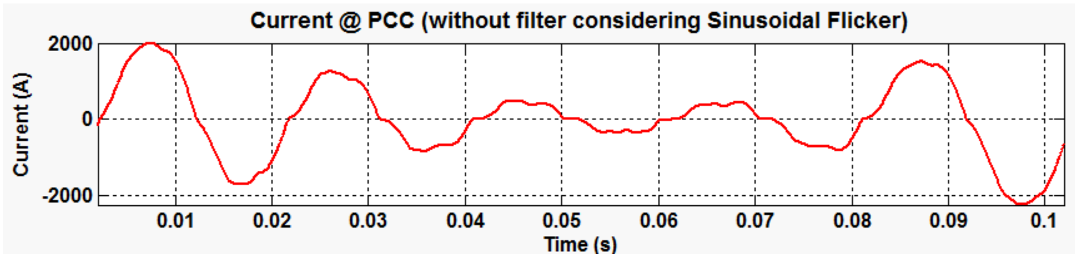

(a)

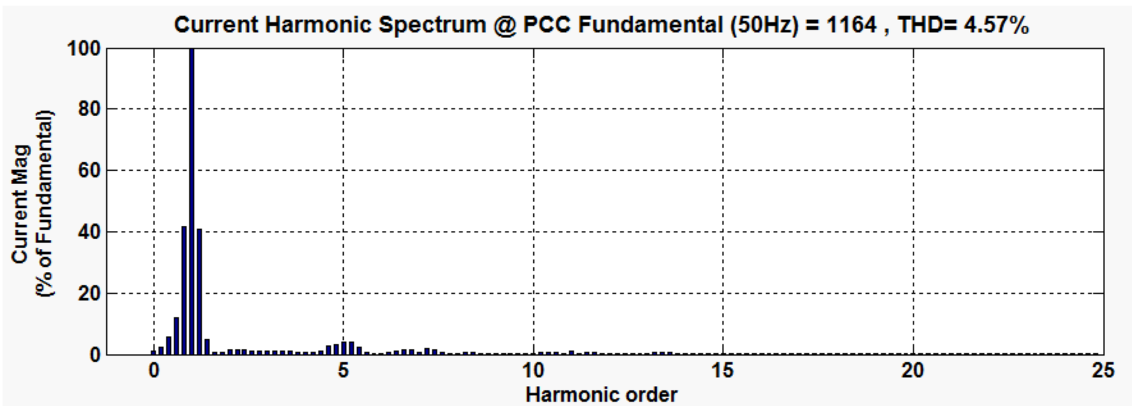

(b)

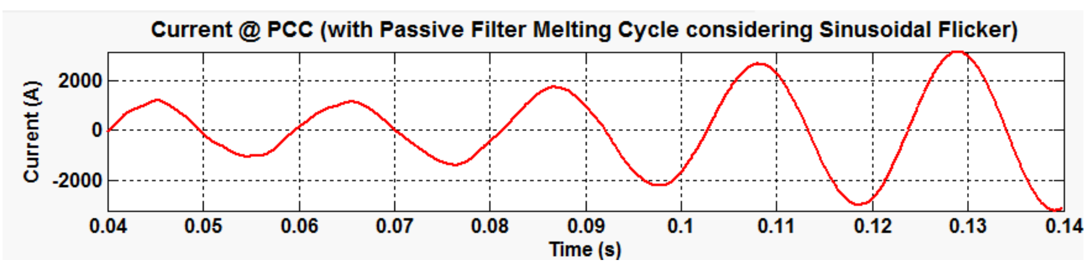

(c)

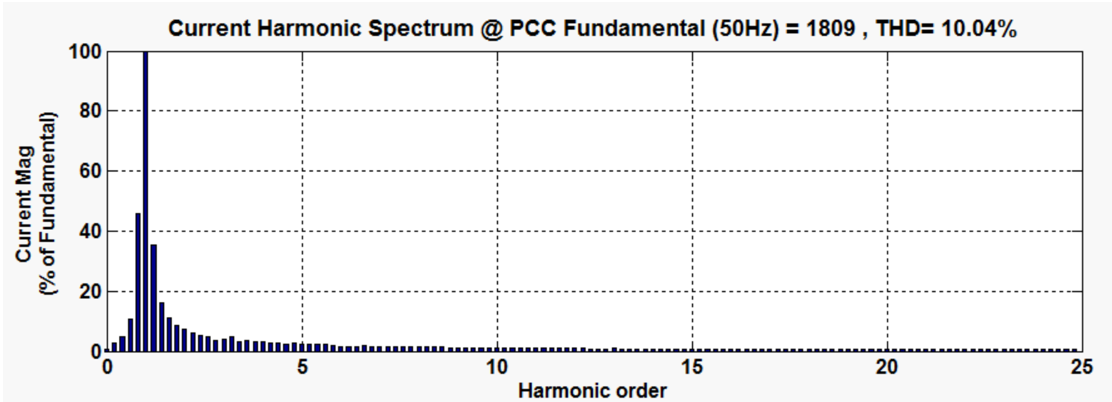

(d)

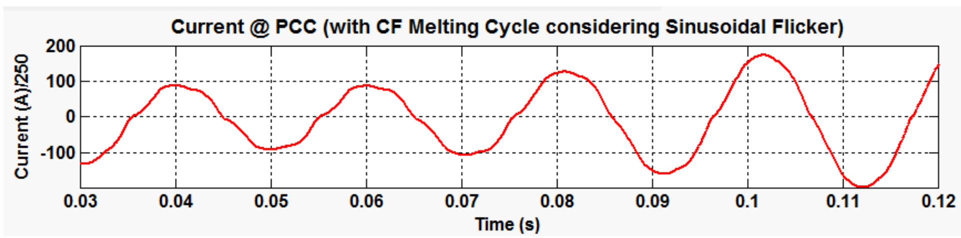

(e)

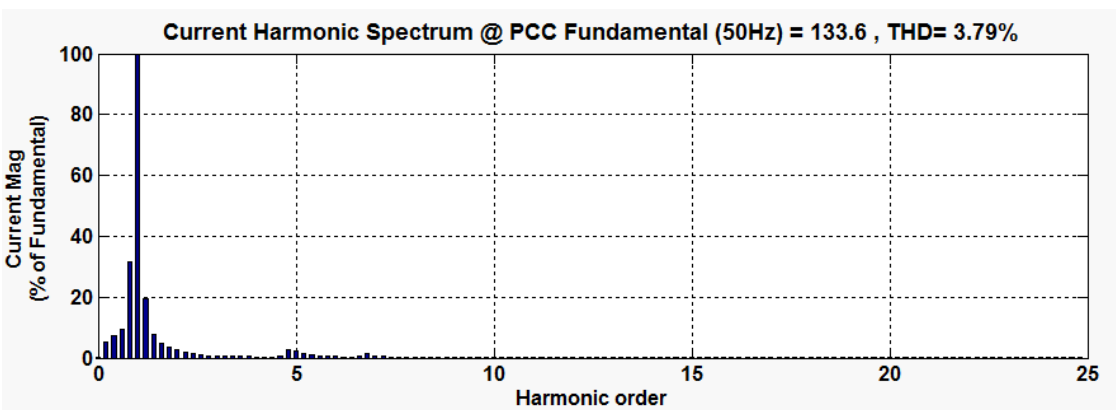

(f)

Figure 5.6 Filter performance in EAF melting cycle considering random flicker (a) I_{PCC} without filter (b) harmonic spectrum without filter (c) I_{PCC} with PF (d) harmonic spectrum with PF (e) I_{PCC} with CF (f) harmonic spectrum with CF

The total harmonic distortion of current (THD_I) observed at PCC is 4.57 % without filter in refining cycle of EAF connected distribution network as shown in Figure 5.3 (b). It has changed to 10.04 % after PF application as shown in Figure 5.6 (d), which is violating

IEEE 519-1992. That means PF is detuned and its performance has deteriorated for melting cycle considering sinusoidal flicker of the EAF operation. Application of CF changes to 3.79 % as shown in Figure 5.6 (f), which are within the permissible limits.

Table 5.3 Harmonic analysis of EAF connected distribution network in melting cycle (sinusoidal flicker)

Parameters/condition	Phase	V/I	THD (%)	RMS	Fund.	H_5 (%)	H_7 (%)	H_{11} (%)	H_{13} (%)
Without filter	Phase-a	V	7.85	6970	9856	6.63	1.63	2.83	0
		I	4.57	823.2	1164	3.95	0	0	0
	Phase-b	V	8.29	6937	9811	6.83	1.56	3.13	1.1
		I	6.62	787.7	1114	4.91	1.17	0	0
	Phase-c	V	8.65	6956	9838	7.03	1.89	2.74	1.02
		I	6.98	817.9	1157	3.74	0	0	0
With PF	Phase-a	V	3.79	5999	8484	0.76	0.19	0.1	0
		I	10.04	1279	1809	2.36	0	0	0
	Phase-b	V	5.5	6150	8697	0.86	0.63	0.48	0
		I	7.43	1280	1810	1.55	0	0	0
	Phase-c	V	6.32	5997	8482	1.11	0.83	0.57	0.76
		I	5.48	1236	1748	0.96	0	0	0
With CF	Phase-a	V	1.27	8084	11430	0.39	0.14	0.07	0.04
		I	5.02	96.78	136.9	2.32	0.25	0.41	0.39
	Phase-b	V	1.36	8090	11440	0.34	0.11	0.09	0.07
		I	4.36	96.61	136.6	1.42	0.68	0.56	0.35
	Phase-c	V	1.35	8089	11440	0.38	0.13	0.09	0.08
		I	3.79	94.49	133.6	2.37	0.53	0.21	0.2

Harmonics spectrum quantified detail is tabulated in Table 5.2. That means PF performs better than CF in reducing THD_I in melting cycle (sinusoidal flicker).

Figure 5.7 (a)-(c)-(e) depicts typical VICs without filter, with PF and with CF application respectively. Figure 5.4 (b)-(d)-(f) shows active-reactive power consumption at PCC by the EAF without filter, with PF and with CF application respectively.

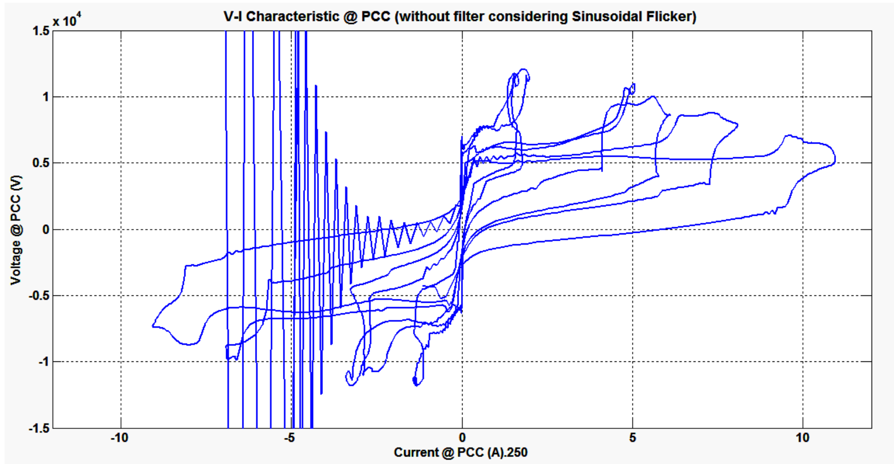

(a)

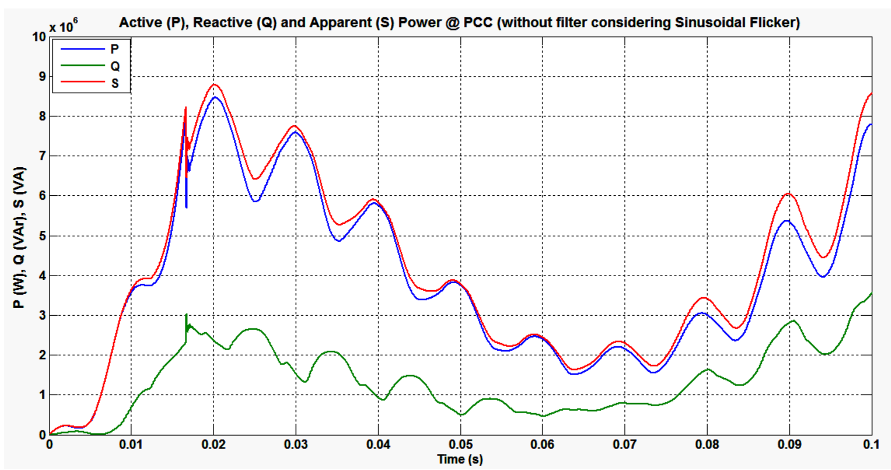

(b)

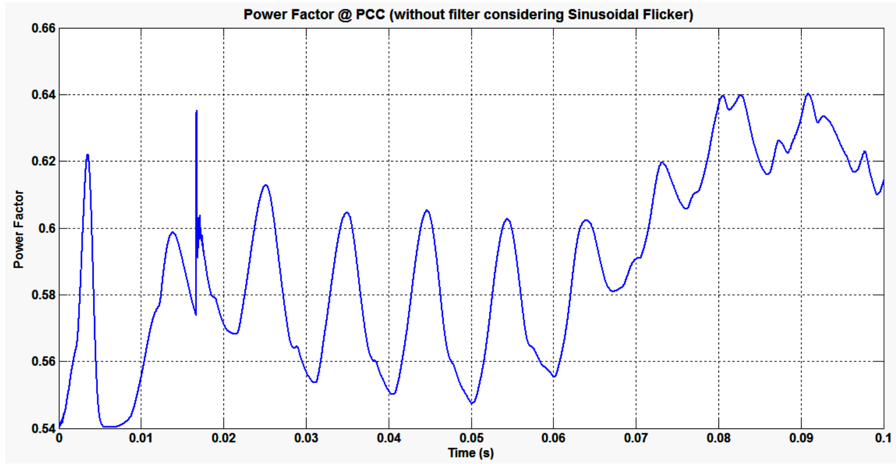
Power Factor @ PCC (without filter considering Sinusoidal Flicker)
Power Factor
Time (s)

(c)

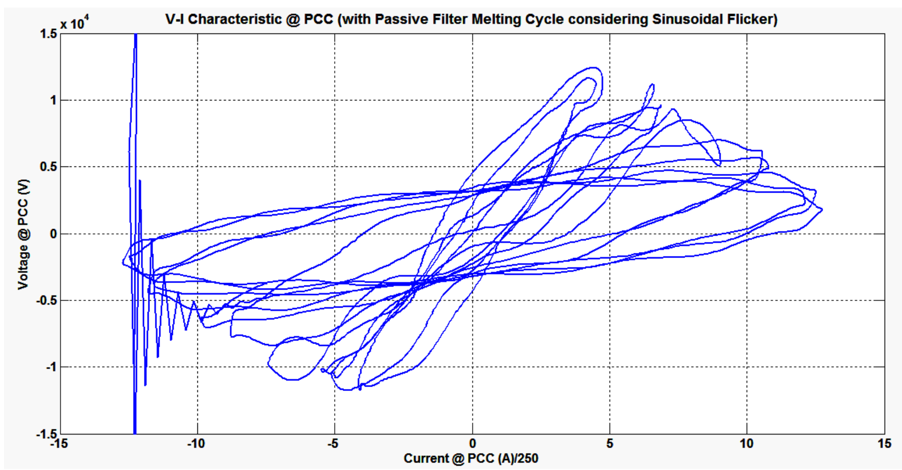
V-I Characteristic @ PCC (with Passive Filter Melting Cycle considering Sinusoidal Flicker)
Voltage @ PCC (V)
Current @ PCC (A)/250

(d)

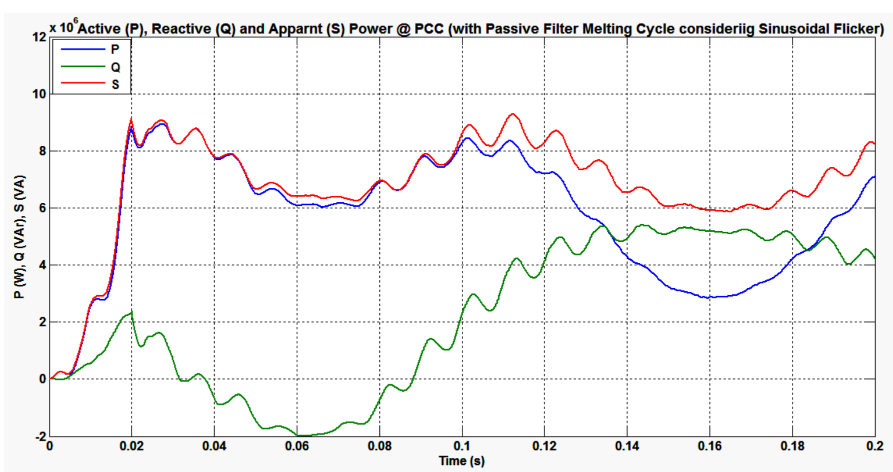
Active (P), Reactive (Q) and Apparnt (S) Power @ PCC (with Passive Filter Melting Cycle consideriig Sinusoidal Flicker)
P
Q
S
P (W), Q (VAr), S (VA)
Time (s)

(e)

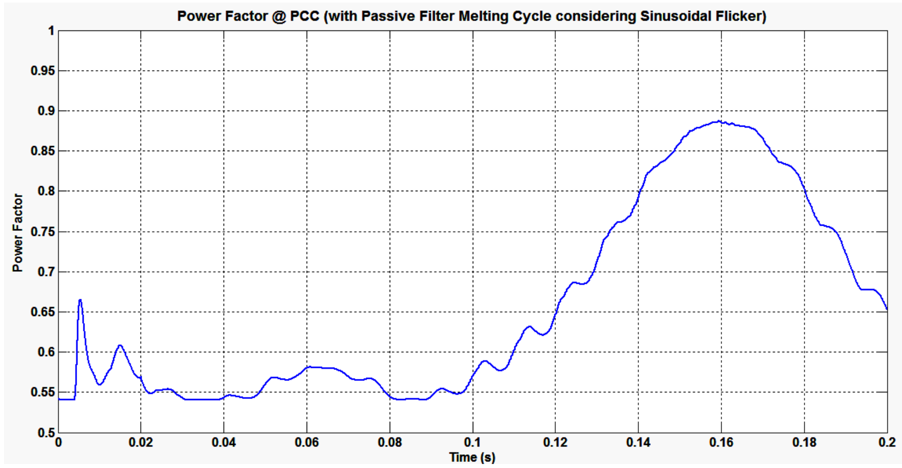
Power Factor @ PCC (with Passive Filter Melting Cycle considering Sinusoidal Flicker)
Power Factor
Time (s)
1
0.95
0.9
0.85
0.8
0.75
0.7
0.65
0.6
0.55
0.5
0
0.02
0.04
0.06
0.08
0.1
0.12
0.14
0.16
0.18
0.2

(f)

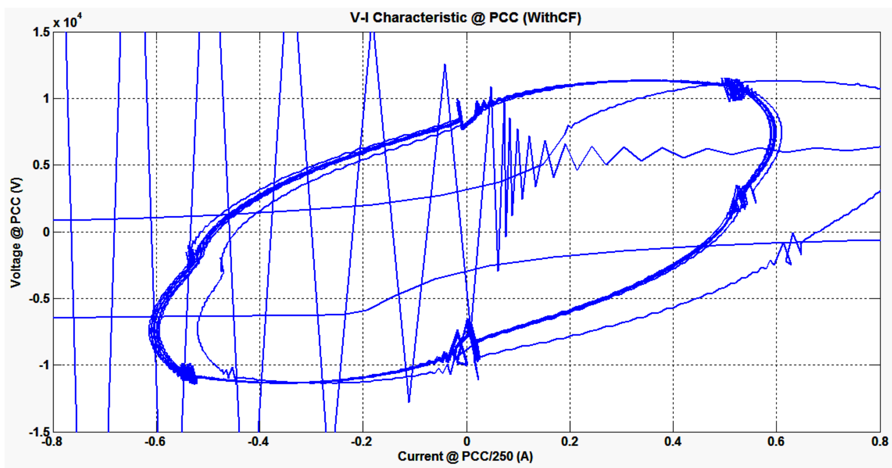
V-I Characteristic @ PCC (WithCF)
x 10^4
Voltage @ PCC (V)
Current @ PCC/250 (A)
1.5
1
0.5
0
-0.5
-1
-1.5
-0.8
-0.6
-0.4
-0.2
0
0.2
0.4
0.6
0.8

(g)

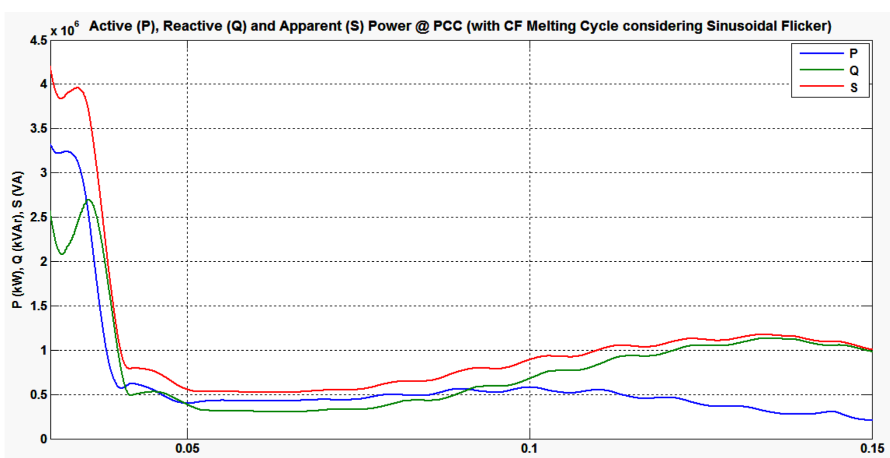
x 10^6 Active (P), Reactive (Q) and Apparent (S) Power @ PCC (with CF Melting Cycle considering Sinusoidal Flicker)
P (kW), Q (kVAr), S (VA)
Time (s)
P
Q
S
4.5
4
3.5
3
2.5
2
1.5
1
0.5
0
0.05
0.1
0.15

(h)

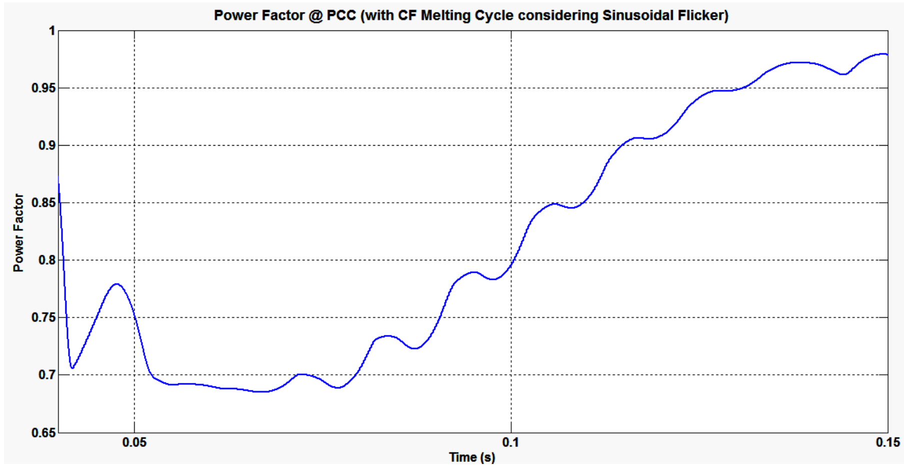

(i)

Figure 5.7 Filter performance in EAF melting cycle considering sinusoidal flicker (a) VIC without filter (b) PQS powers without filter (c) power factor without filter (d) VIC with PF (e) PQS powers with PF (f) power factor with PF (g) VIC with CF (h) PQS powers with CF (i) power factor with CF

Figure 5.7 (c)-(f)-(i) shows power factor variation without filter, with PF and with CF application respectively at PCC. Table 5.4 shows tabulated values of active-reactive-apparent power and power factor after PF and CF application.

Table 5.4 Power analysis in melting cycle (sinusoidal flicker)

Parameters/condition	Phase	P (kW)	Q (kVAr)	S (kVA)	pf
Without filter	Phase-a	4771	2485	5448	0.62
	Phase-b	4772	2495	5454	0.62
	Phase-c	4769	2495	5452	0.62
With PF	Phase-a	6862	1138	7433	0.59
	Phase-b	6955	1092	7531	0.59
	Phase-c	6904	1193	7472	0.59
With CF	Phase-a	6658	1020	7435	0.86
	Phase-b	8193	1145	7471	0.86
	Phase-c	7209	1137	8489	0.86

It can be seen from Table 5.4 that the power factor without filter is 0.59 which is improved to 0.62 and later to 0.86 after PF and CF application respectively in melting cycle (sinusoidal flicker) of the EAF distribution network at PCC. It means CF performs better than PF alone in power factor improvement.

5.2.3 Performance analysis of CF in melting cycle (random flicker)

Figure 5.8 shows filter performance in melting cycle considering random flicker of the EAF connected distribution network. Figure 5.8 (a)-(c)-(e) shows V_{PCC} waveforms without filter, with PF and with CF respectively. Figure 5.8 (b)-(d)-(f) shows harmonic spectrum of V_{PCC} without filter, with PF and with CF respectively.

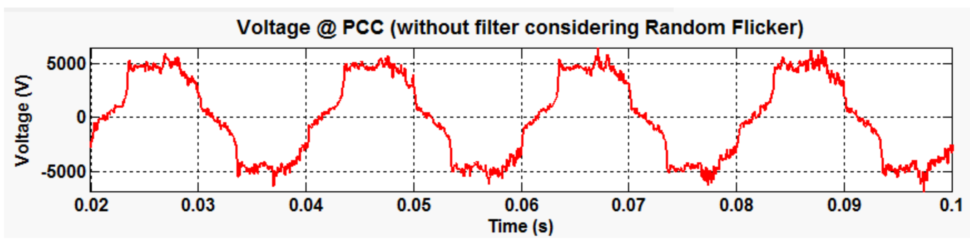

(a)

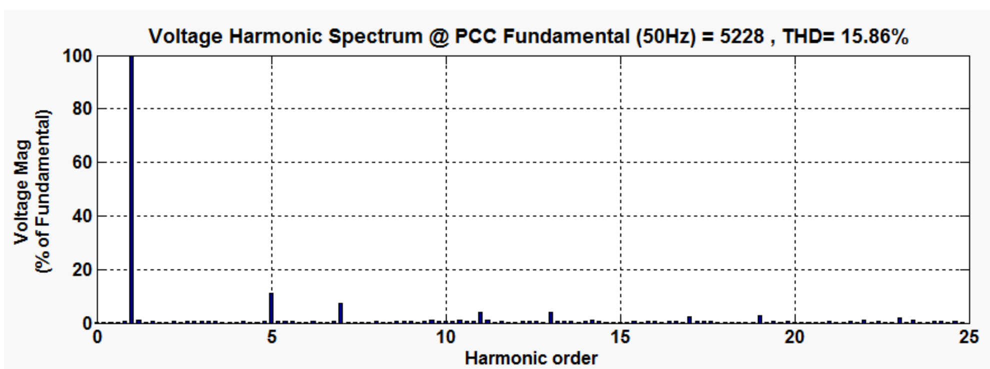

(b)

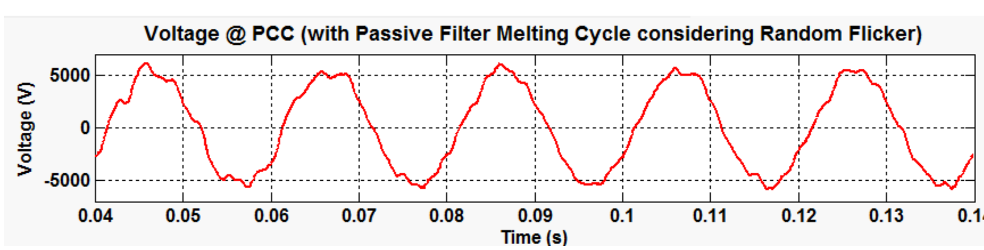

(c)

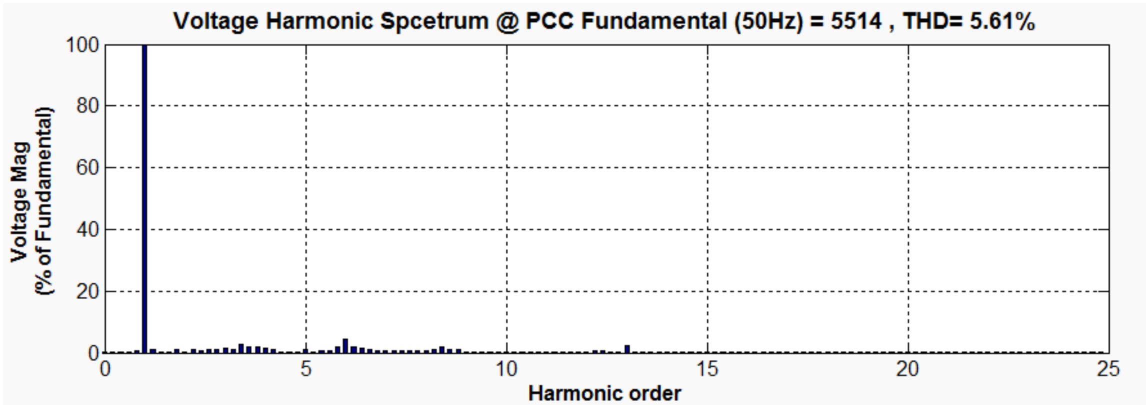

(d)

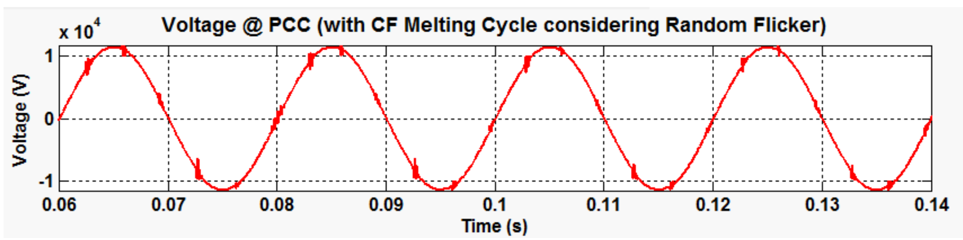

(e)

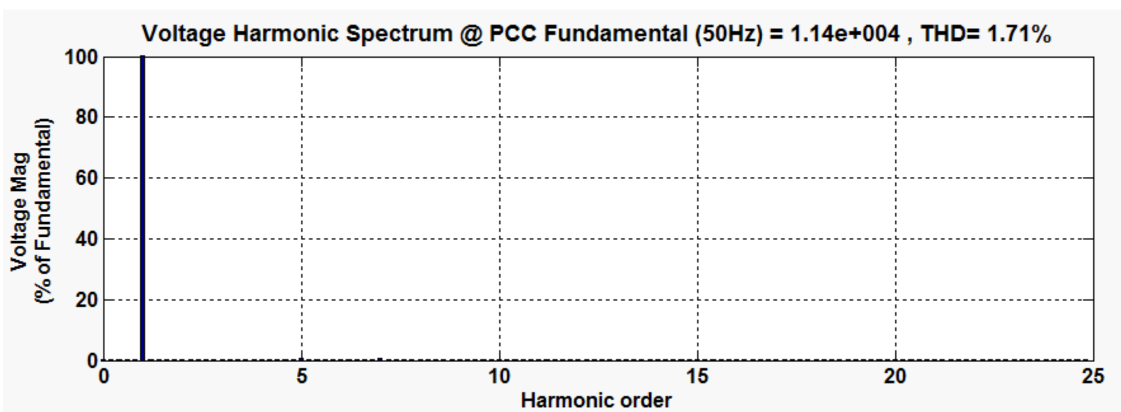

(f)

Figure 5.8 Filter performance in EAF melting cycle (random flicker) (a) V_{PCC} without filter (b) harmonic spectrum without filter (c) V_{PCC} with PF (d) harmonic spectrum with PF (e) V_{PCC} with CF (f) harmonic spectrum with CF

The total harmonic distortion of voltage (THD_V) observed at PCC is 15.86 % without filter in melting cycle considering random flicker of EAF connected distribution network as shown in Figure 5.8 (b). This value is violating IEEE 519-1992 limits. It should be below

5%. That is improved to 5.61 % after passive filter application as shown in Figure 5.8 (d), which is nearer to the IEEE 519-1992 limit of 5 % but little more than the required. An application of CF changes THD_V to 1.71 % as shown in Figure 5.8 (f). That means CF performs better than PF in improving THD_V in melting cycle considering sinusoidal flicker of EAF connected distribution network.

Table 5.5 show three phase harmonic spectrum details of voltage and current at PCC for melting cycle considering random flicker of the EAF connected distribution network.. It can be seen that 5^{th}, 7^{th}, 11^{th} and 13^{th} are the major harmonic components present in voltage at PCC and are more than IEEE 519-1992 limit of 5 % of harmonic distortion. It can be seen from Table 5.5 that both PF and CF can suppress individual harmonic components within the limit in refining cycle of EAF distribution network at PCC but CF performs better than the PF.

Figure 5.9 shows filter performance in melting cycle considering random flicker of the EAF connected network. Figure 5.9 (a)-(c)-(e) shows I_{PCC} waveforms without filter, with PF and with CF respectively. Figure 5.9 (b)-(d)-(f) shows harmonic spectrum of I_{PCC} without filter, with PF and with CF respectively.

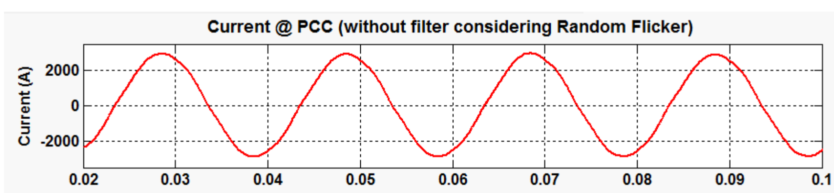

(a)

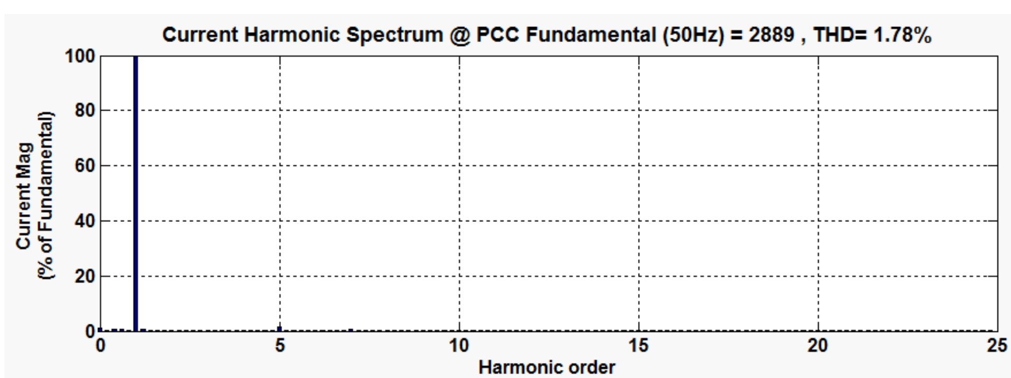

(b)

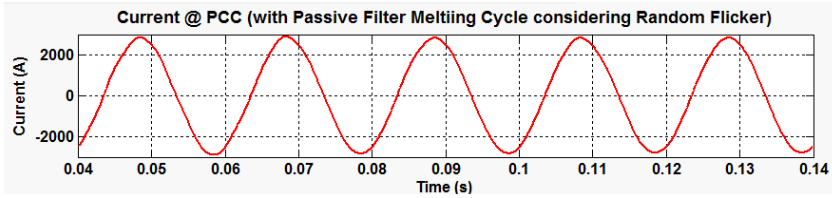

(c)

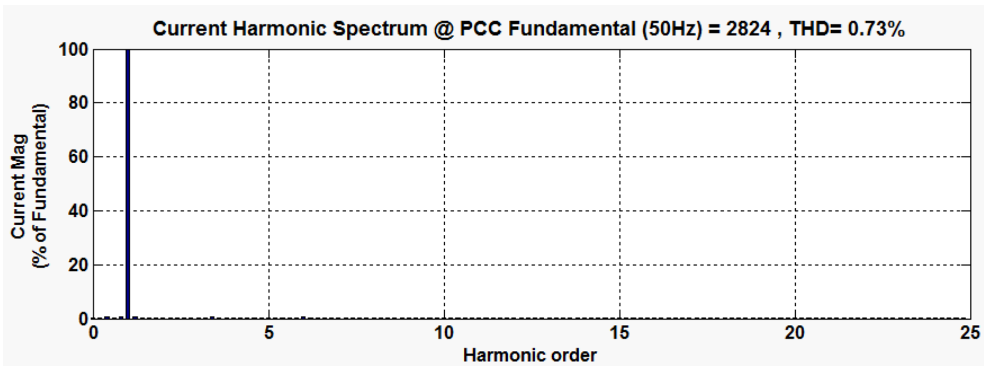

(d)

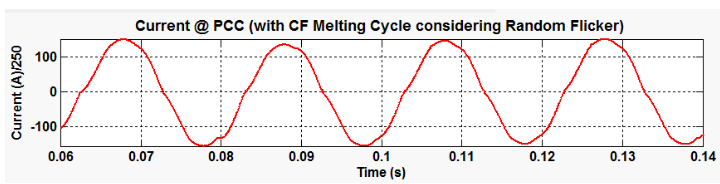

(e)

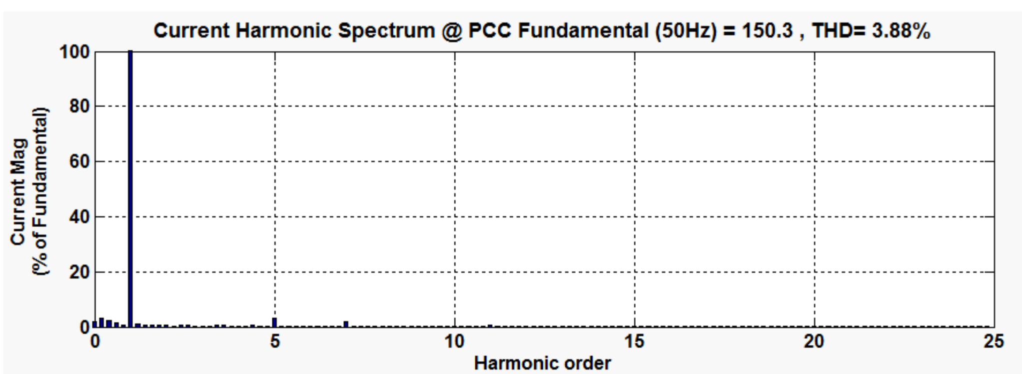

(f)

Figure 5.9 Filter performance in EAF melting cycle considering random flicker (a) I_{PCC} without filter (b) harmonic spectrum without filter (c) I_{PCC} with PF (d) harmonic spectrum with PF (e) I_{PCC} with CF (f) harmonic spectrum with CF

The total harmonic distortion of current (THD_I) observed at PCC is 1.78 % without filter in refining cycle of EAF connected distribution network as shown in Figure 5.9 (b), which is within the IEEE 519-1992 limit of 5%.It has changed to 0.73 and then to 3.88 % after PF and CF application as shown in Figure 5.9 (d) and Figure 5.9 (f) respectively. Harmonics spectrum quantified detail is tabulated in Table 5.5.

Table 5.5 Harmonic analysis of EAF connected distribution network in melting cycle (random flicker)

Parameters/condition	**Phase**	**V/I**	**THD (%)**	**RMS**	**Fund.**	**H_5 (%)**	**H_7 (%)**	**H_{11} (%)**	**H_{13} (%)**
Without filter	Phase-a	V	15.86	3697	5228	11	7.48	4.06	4.1
		I	1.78	2043	2889	1.51	0	0	0
	Phase-b	V	15.98	3687	5214	11.29	7.62	4.21	3.32
		I	1.82	2035	2878	1.58	0	0	0
	Phase-c	V	15.63	3706	5241	10.69	7.86	4.05	0
		I	1.77	2028	2868	1.43	0	0	0
With PF	Phase-a	V	5.61	3899	5514	0.89	0.67	0.03	2.33
		I	0.73	1997	2824	0.12	0	0	0
	Phase-b	V	4.65	3886	5496	1.12	0.22	0.12	1.99
		I	0.72	1997	2824	0.15	0	0	0
	Phase-c	V	3.45	3903	5519	0.97	0.45	0.1	1.7
		I	0.64	1992	2818	0.05	0	0	0
With CF	Phase-a	V	1.71	8064	1140	0.65	0.42	0.22	0.19
		I	3.88	16.3	150.4	3.32	1.69	0.53	0.3
	Phase-b	V	1.92	8067	11410	0.68	0.43	0.25	0.15
		I	4.32	105.3	149.6	3.72	1.73	0.6	0.36
	Phase-c	V	1.92	8068	1140	0.66	0.42	0.25	0.14
		I	4.27	106.1	149.7	3.5	1.74	0.68	0.28

Figure 5.10 (a)-(c)-(e) depicts typical VICs without filter, with PF and with CF application respectively. Figure 5.10 (b)-(d)-(f) shows active-reactive power consumption at PCC by the EAF without filter, with PF and with CF application respectively.

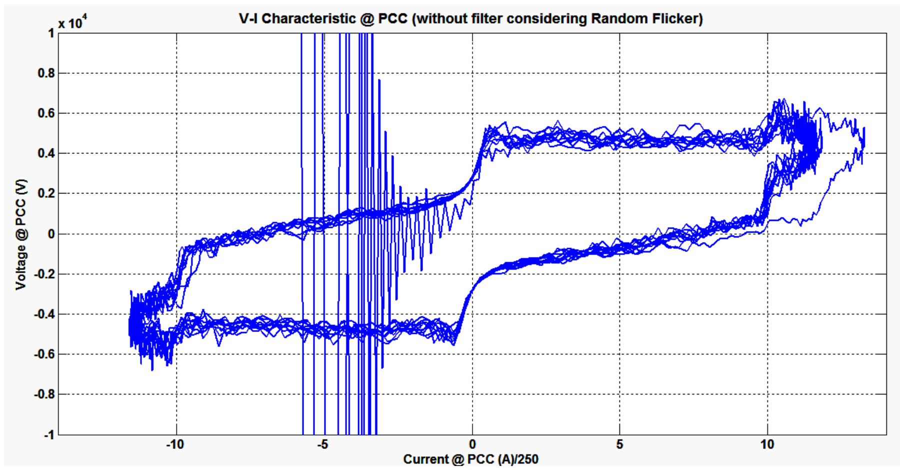

(a)

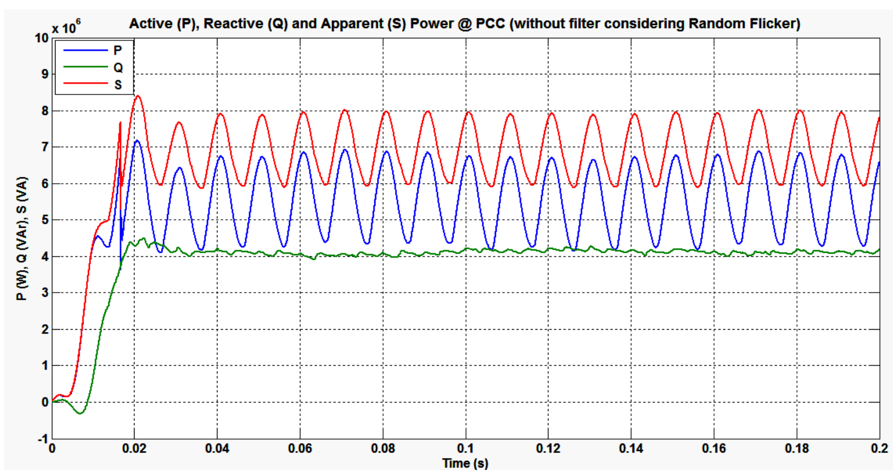

(b)

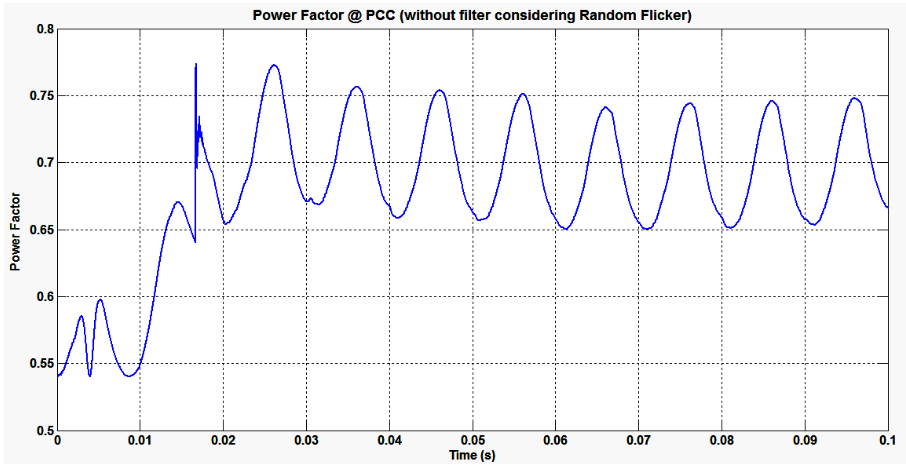
Power Factor @ PCC (without filter considering Random Flicker)
Power Factor
Time (s)

(c)

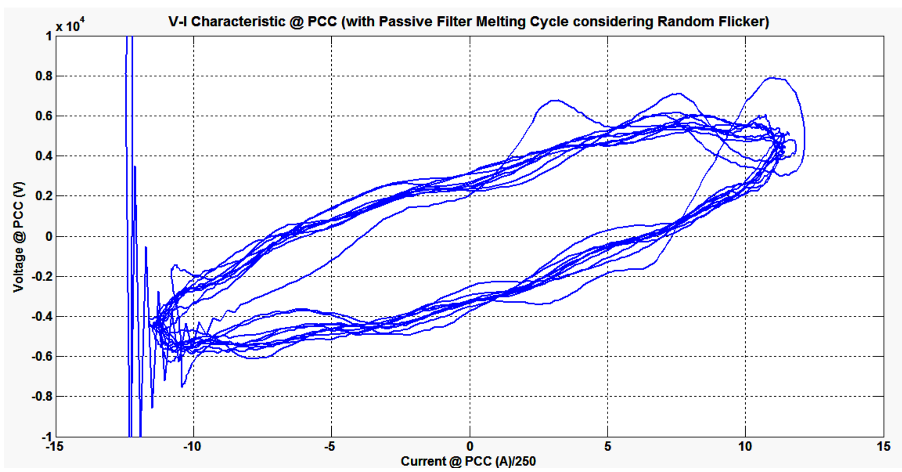
V-I Characteristic @ PCC (with Passive Filter Melting Cycle considering Random Flicker)
x 10^4
Voltage @ PCC (V)
Current @ PCC (A)/250

(d)

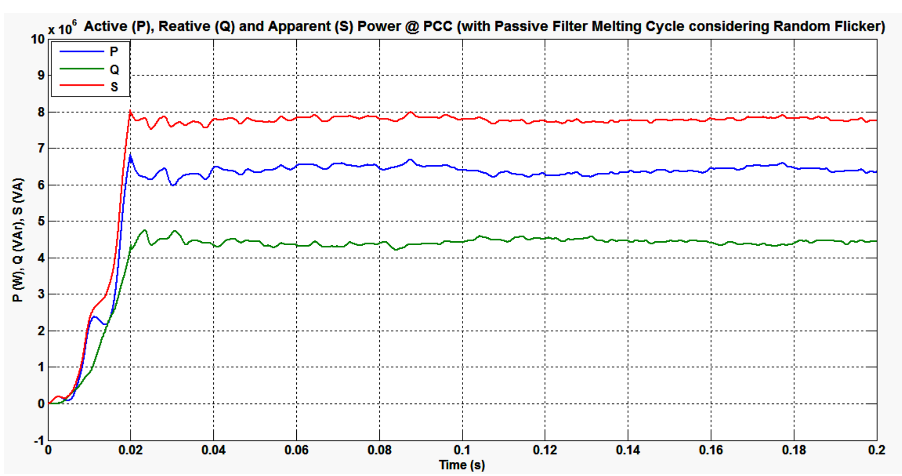
x 10^6 Active (P), Reative (Q) and Apparent (S) Power @ PCC (with Passive Filter Melting Cycle considering Random Flicker)
P
Q
S
P (W), Q (VAr), S (VA)
Time (s)

(e)

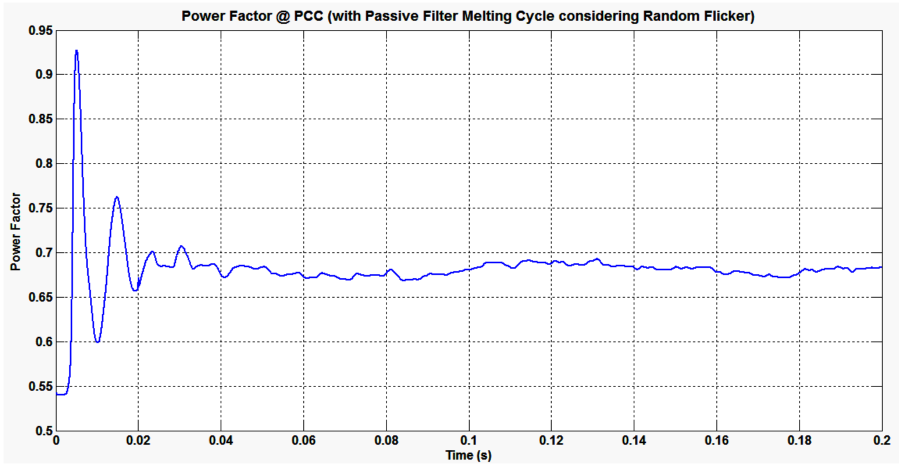
Power Factor @ PCC (with Passive Filter Melting Cycle considering Random Flicker)
Power Factor
Time (s)

(f)

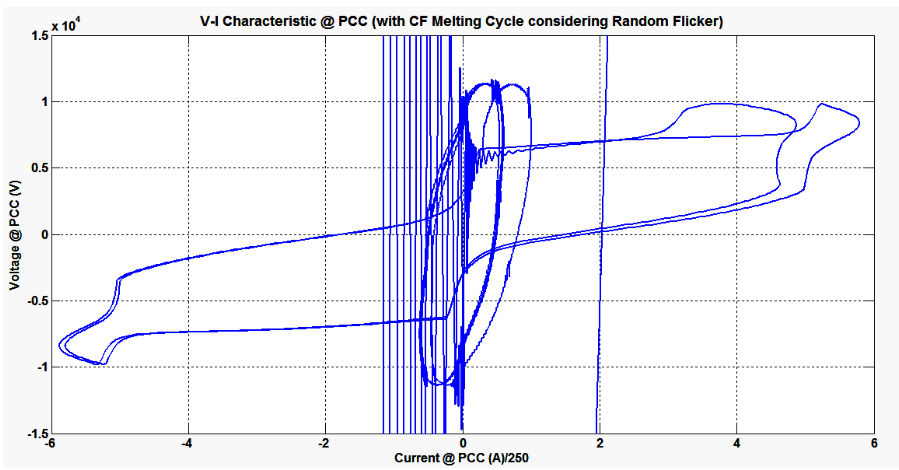
V-I Characteristic @ PCC (with CF Melting Cycle considering Random Flicker)
x 10^4
Voltage @ PCC (V)
Current @ PCC (A)/250

(g)

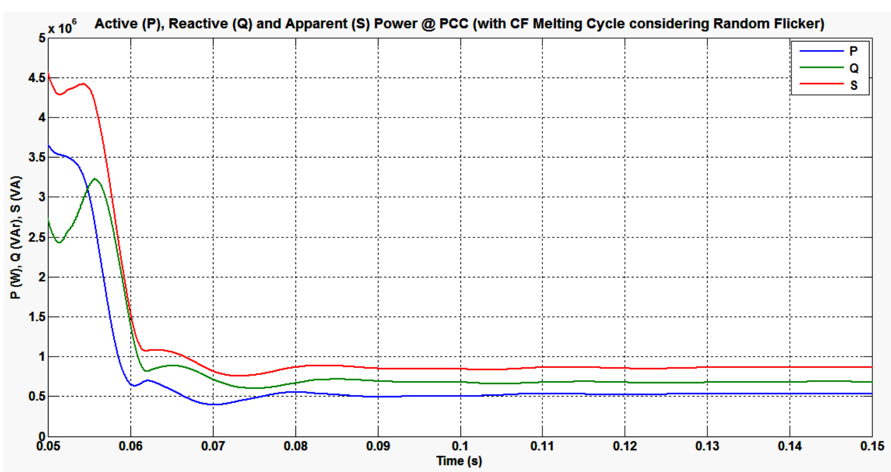
Active (P), Reactive (Q) and Apparent (S) Power @ PCC (with CF Melting Cycle considering Random Flicker)
x 10^6
P (W), Q (VAr), S (VA)
P
Q
S
Time (s)

(h)

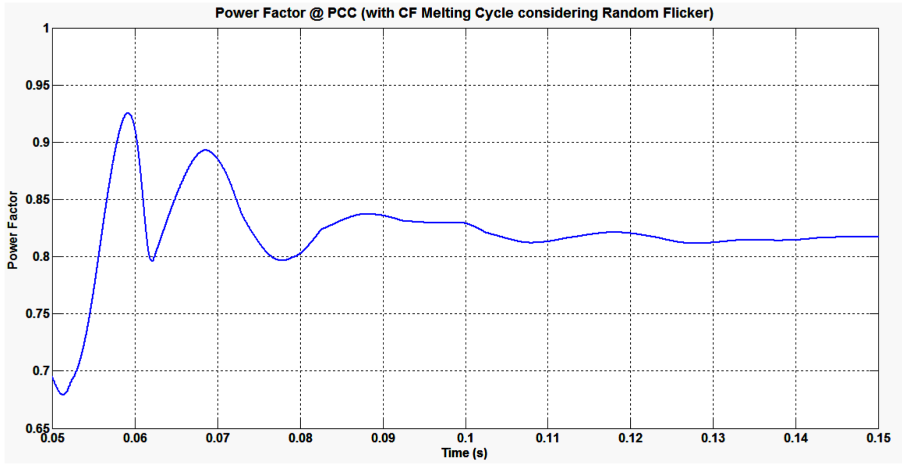

(i)

Figure 5.10 Filter performance in EAF melting cycle considering random flicker (a) VIC without filter (b) PQS powers without filter (c) power factor without filter (d) VIC with PF (e) PQS powers with PF (f) power factor with PF (g) VIC with CF (h) PQS powers with CF (i) power factor with CF

Figure 5.10 (c)-(f)-(i) shows power factor variation without filter, with PF and with CF application respectively at PCC. Table 5.6 shows tabulated values of active-reactive-apparent power and power factor after PF and CF application.

Table 5.6 Power analysis in melting cycle (random flicker)

Parameters/condition	Phase	P (kW)	Q (kVAr)	S (kVA)	pf
Without filter	Phase-a	6028	4552	7554	0.69
	Phase-b	6000	4560	7536	0.69
	Phase-c	6013	4561	7547	0.69
With PF	Phase-a	6406	4424	7786	0.68
	Phase-b	6342	4454	7752	0.68
	Phase-c	6371	4453	7774	0.68
With CF	Phase-a	5227	6945	8701	0.82
	Phase-b	5718	7195	9238	0.81
	Phase-c	5263	7416	9183	0.82

It can be seen from Table 5.6 that the power factor without filter is 0.68 which is improved to 0.69 and later to 0.82 after PF and CF application respectively in melting cycle (random flicker) of the EAF distribution network at PCC. It means CF performs better than PF alone in power factor improvement.

Figure 5.11 shows three phase voltages at PCC under refining cycle condition of EAF connected distribution network.

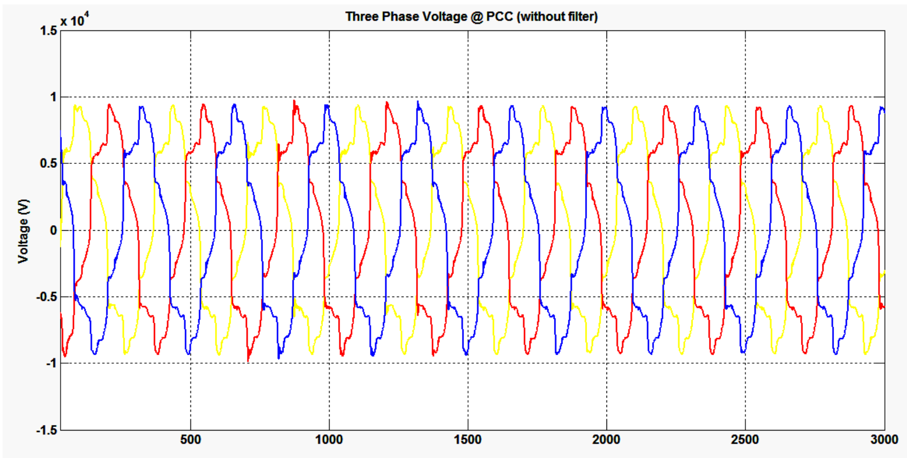

(a)

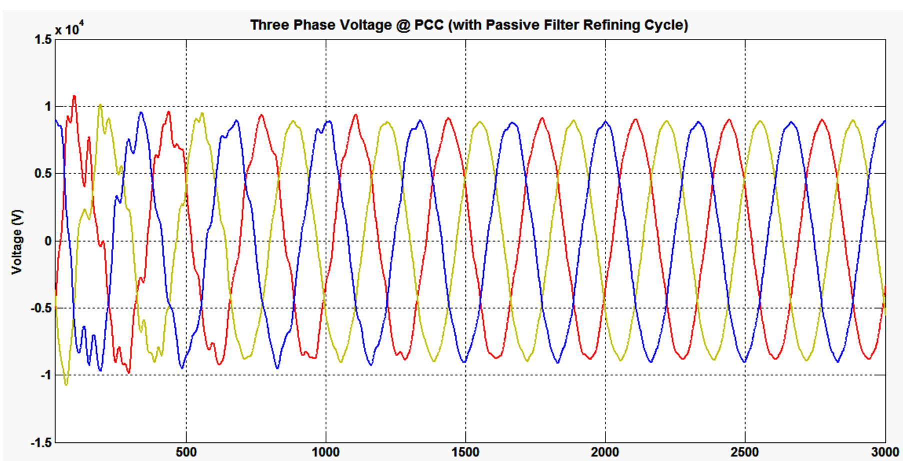

(b)

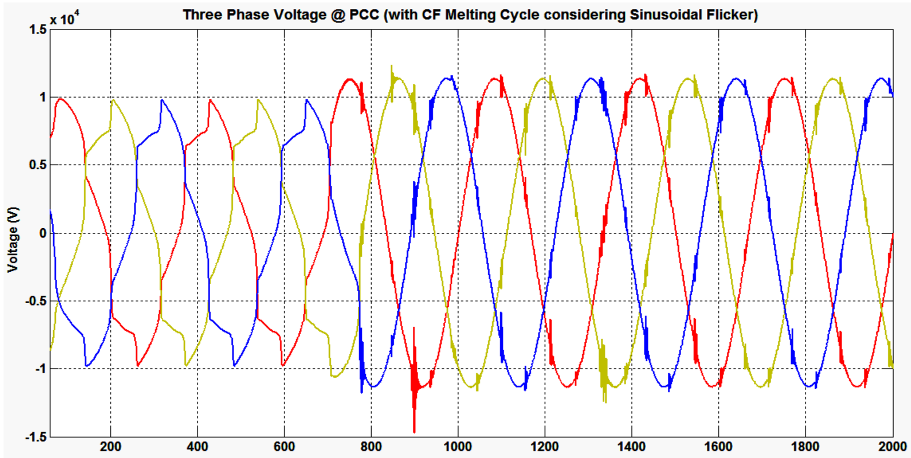

(c)

Figure 5.11 Three phase V_{PCC} for refining cycle (a) without filter (b) with PF (c) with CF

Figure 5.11 (a)-(b)-(c) shows three-phase V_{PCC} without filter, with PF and with CF application respectively at PCC.

Figure 5.12 (a)-(b)-(c) shows three-phase V_{PCC} without filter, with PF and with CF application respectively at PCC under melting cycle considering sinusoidal flicker of EAF connected distribution network.

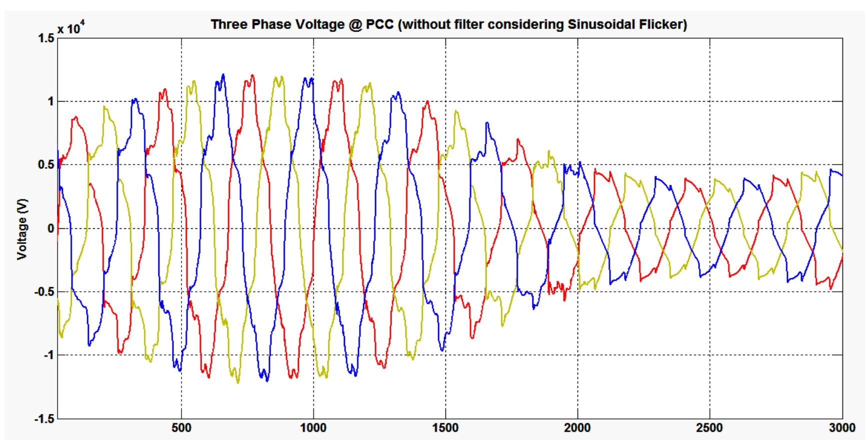

(a)

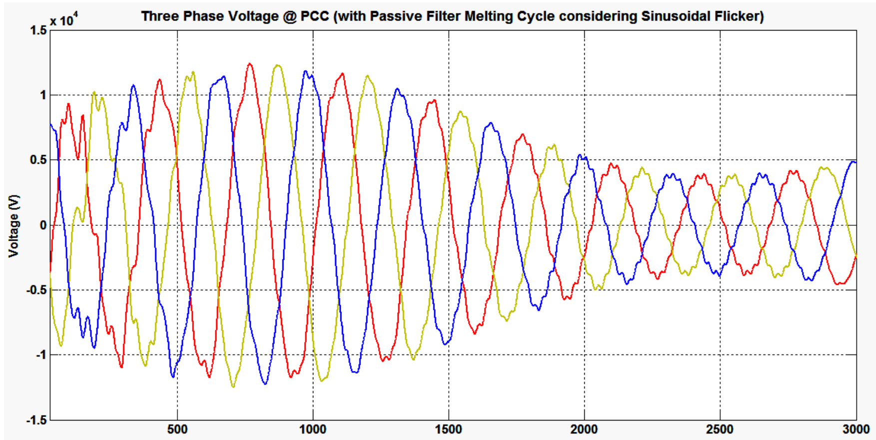

(b)

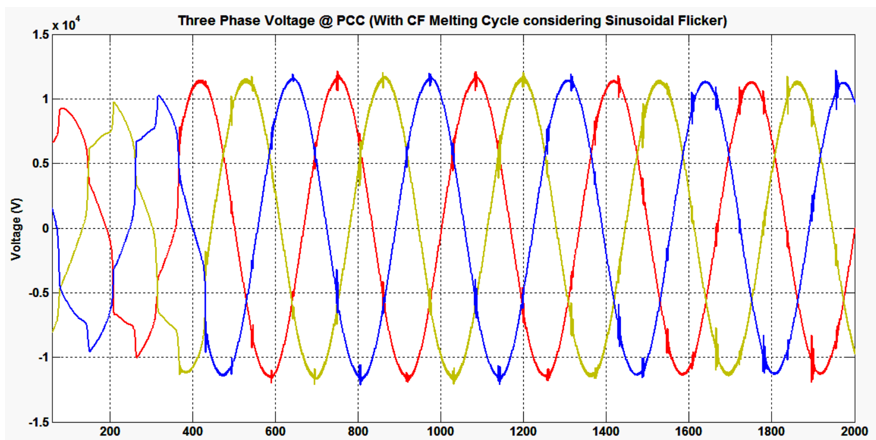

(c)

Figure 5.12 Three phase V_{PCC} for sinusoidal flicker (a) without filter (b) with PF (c) with CF

Comparison of Figure 5.12 (b) and Figure 5.11 (c) itself concludes better performance of CF than PF in removing sinusoidal flicker.

% Voltage flicker for sinusoidal variation is estimated using equation (2.16) for passive filter and composite filter application as shown in Table 5.7.Tabulated results and Figure 5.4 clearly show that the passive filter fails to clear sinusoidal voltage flicker whereas composite filter reduces voltage flicker from 2.92 % to 1.78 %. For 4 Hz of frequency pulsation applied and for 1.29 of % voltage pulsation (% voltage flicker) with composite filter, the operating point lies in non-perceptible zone as per the Fig. 5. Which means composite filter brings voltage flicker in within non-perceptible criteria.

Table 5.7 Voltage flicker analysis

Parameters	**Without Filter**	**With PF**	**With CF**
Voltage Measurement			
V_{1P} (V)	5343	5621	3243
V_{2P} (V)	10900	11490	11590
% Flicker Calculation			
% Voltage Flicker	2.92	2.92	1.78

Figure 5.13 (a)-(b)-(c) shows three-phase V_{PCC} without filter, with PF and with CF application respectively at PCC under melting cycle considering random flicker of EAF connected distribution network.

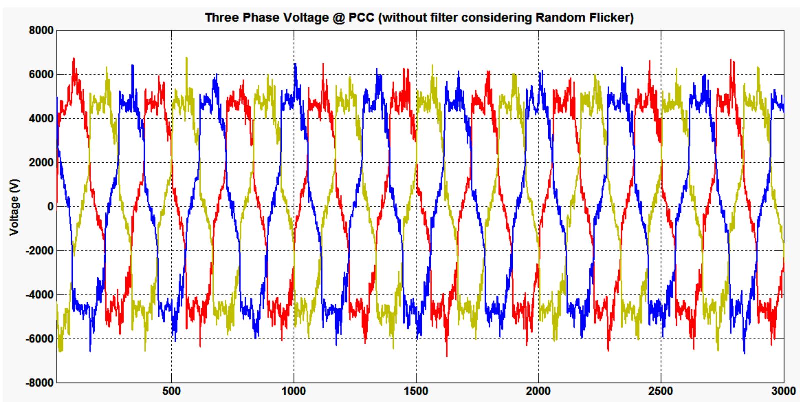

(a)

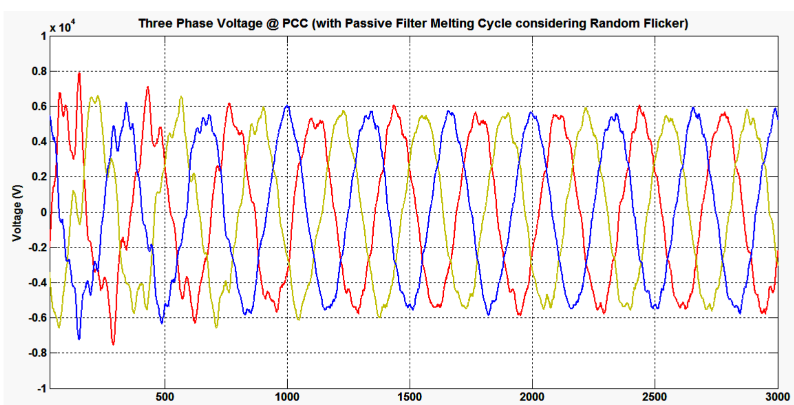

(b)

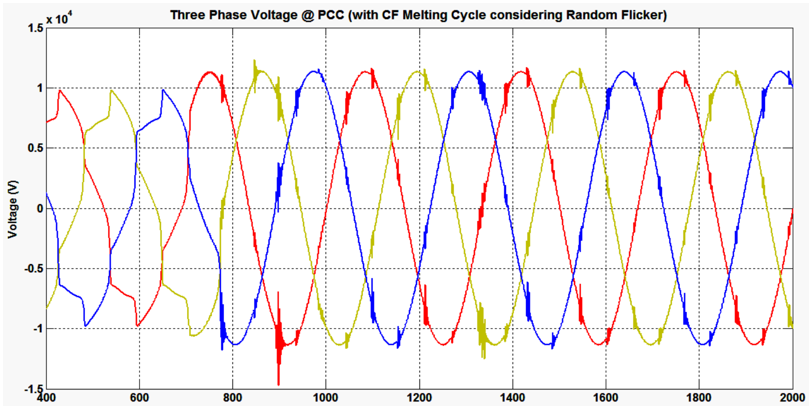

(c)

Figure 5.13 Three phase V_{PCC} for random flicker (a) without filter (b) with PF (c) with CF

Comparison of Figure 5.13 (b) and Figure 5.13 (c) itself concludes better performance of CF than PF in removing random flicker.

5.2.4 Performance analysis of CF in voltage unbalance

Unbalance voltage condition is simulated by varying values of E_0 in case of Cassie-Mayr's EAF model where as V_{at0} in case of the proposed EAF model as per Table 5.8.

Table 5.8 Voltage unbalances condition parameters

Parameter	EAF Model 1 (Cassie-Mayr)	EAF Model 2 (Proposed)
E_0=V_{at0} for a-Phase	250	250
E_0=V_{at0} for b-Phase	300	300
E_0=V_{at0} for c-Phase	350	350

Simulated three phase voltage at PCC for voltage unbalance case has been shown in Figure 5.14.

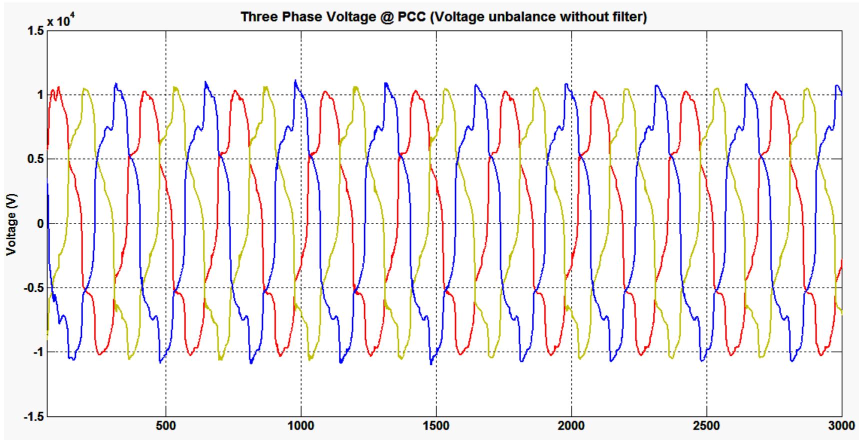

(a)

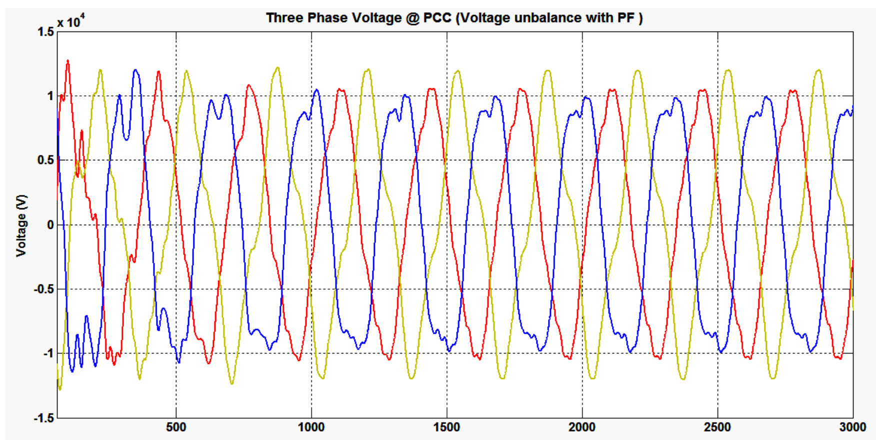

(b)

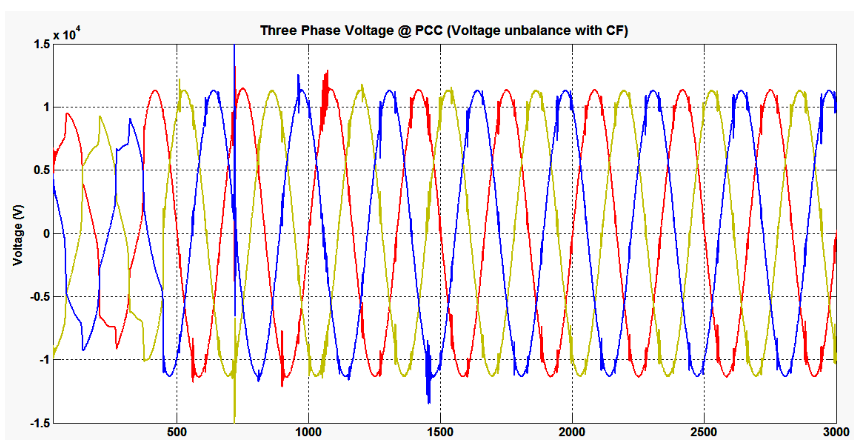

(c)

Figure 5.14 Three phase voltage unbalance (a) without filter (b) with PF (c) with CF

The reflected phase voltage values both-peak and RMS are tabulated in Table 5.9.

Table 5.9 Voltage unbalances analysis

Without Filter				
Parameter	**Peak**	**RMS**	**Voltage Unbalance (Peak)**	**% Unbalance (Peak)**
Voltage Phase-a	9140	6463	106.30	6.31
Voltage Phase-b	8661	6124	100.73	0.73
Voltage Phase-c	7993	5652	92.96	-7.03
Voltage (Average)	8598.00	6079.67		
Voltage (Average Deviation)	403.33	285.11		
Voltage (% Average Deviation)	4.69	4.69		
With Passive Filter				
Voltage Phase-a	9632	6811	106.72	6.72
Voltage Phase-b	8946	6326	99.12	-0.88
Voltage Phase-c	8498	6009	94.16	-5.84
Voltage (Average)	9025.33	6382.00		
Voltage (Average Deviation)	404.44	286.00		
Voltage (% Average Deviation)	4.48	4.48		
With Composite Filter				
Voltage Phase-a	11420	8078	100.41	0.45
Voltage Phase-b	11350	8025	99.79	-0.21
Voltage Phase-c	11350	8022	99.79	-0.24
Voltage (Average)	11373	8041.7		
Voltage (Average Deviation)	31.11	24.22		
Voltage (% Average Deviation)	0.27	0.30		

From these values, average voltage deviation and per phase voltage deviation is calculated for peak and RMS values. It can be seen from Table 5.7 that the voltage unbalance has improved to 0.27 % from 4.69 % on an average.

5.3 Performance evaluation of CF

Performances of PF and CF for various operational cycles of EAF distribution network has been analyzed in this section. Table 5.10 shows percentage improvement in the respective voltage harmonic components after application of PF and CF. It can also be noted that performance of composite filter is better than the passive filter for H_5 and H_7 components, which are the major concern.

Table 5.10 Filter performance in voltage harmonics reduction

Parameter	Refining cycle		Melting cycle (Sinusoidal flicker)		Melting cycle (Random flicker)	
	With PF	With CF	With PF	With CF	With PF	With CF
H_5 (%)	94.77	94.64	86.68	94.58	90.96	93.97
H_7 (%)	95.87	94.75	65.72	92.52	94.16	94.47
H_{11} (%)	98.74	96.79	86.78	97.13	97.97	94.16
H_{13} (%)	65.96	94.16	64.15	91.04	18.87	93.53
THD_V (%)	74.04	89.37	37.03	83.95	71.12	88.31

Table 5.11 Filter performance in current harmonics reduction

Parameter	Refining cycle		Melting cycle (Sinusoidal flicker)		Melting cycle (Random flicker)	
	With PF	With CF	With PF	With CF	With PF	With CF
H_5 (%)	96.82	47.77	61.35	51.51	92.92	94.9
H_7 (%)	98.21	57.68	100	24.79	100	100
H_{11} (%)	100	78.28	100	100	100	100
H_{13} (%)	100	64.84	100	100	100	100
THD_I (%)	84.86	53.6	-26.31	27.52	61.08	88.18

Table 5.11 shows percentage improvement in the respective current harmonic components after application of PF and CF. It can also be noted that performance of CF is better than the PF for H5 and H7 components, which are the major concern.

Table 5.12 shows percentage improvement in the power factor at PCC after application of PF and CF. It can be seen that performance of CF is better than the PF.

Table 5.12 Filter performance in power factor improvement

Parameter	Refining cycle		Melting cycle (Sinusoidal flicker)		Melting cycle (Random flicker)	
	With PF	With CF	With PF	With CF	With PF	With CF
Power Factor	5.08	38.98	4.84	38.71	1.45	18.84

Table 5.13 shows performance of PF and CF under voltage unbalanced condition. Tabulated results show that PF alone fails to clear voltage unbalance whereas CF performs better than PF.

Table 5.13 Filter performance in voltage unbalance clearance

Parameter	Without filter	With PF	With CF
Peak voltage unbalance (%)	4.69	4.48	93.97
RMS voltage unbalance (%)	4.69	4.48	93.30

Voltage unbalance during arcing is the one of the important phenomenon in EAF. The designed CF has capability of clearing this voltage unbalance as per the tabulated results in Table 5.14, which again confirms better performance of CF in reducing voltage flicker than PF alone.

Table 5.14 Filter performance in reducing voltage flicker

Parameter	Withoutfilter	WithPF	WithCF
% Voltage Flicker	2.92	2.92	1.78
% Improvement	--	0	39.04

5.4 Summary

This chapter describes the simulation and analysis of composite filter for power quality improvement of electric arc furnace distribution network. Distribution network is simulated using Cassie-Mayr and the proposed EAF models. The combined model connected distribution network describes most of the specifications and operational characteristics of EAF. The simulated EAF distribution network is used for power quality analysis-voltage-current harmonics, voltage flicker and voltage unbalance. Next, a control strategy, based on the dual vectorial theory of power, for a composite filter connected in parallel with the unbalance, non-sinusoidal and randomly varying EAF is proposed. Finally, performance of passive filter and series active power filter is compared for various operation cycles of EAFs connected distribution network. Performance comparison shows that, the proposed composite filter performs better than the passive filter alone for harmonic compensation, voltage flicker mitigation, and for clearing voltage unbalance.